Eurasian Chemical Communications

SAMI

FULL PAPER

Synthesis, spectroscopic characterization and thermal study of some transition metal complexes derived from caffeine azo ligand with some of their applications

Noor Adel Hussein | Alyaa Khider Abbas (iD)

Department of Chemistry, College of Science, university of Baghdad, Baghdad, Iraq

Novel N,N-bidentate azo ligand, namely 8-[5-(2-sulfonic acid naphthyl)azo]Caffeine (SNAC), as well as their metal complexes with [Ag(I), Co(II), Cu(II), Pd(II) ,and Pt(IV)] were synthesized and characterized by utilizing elemental analysis, spectroscopic techniques, magnetic susceptibility, molar conductance and thermal analysis. The stability constant and Gibbs free energy were examined by spectroscopic methods. The ligand(SNAC) in comparison to its complexes were tested for their antibacterial, antioxidant , anticancer and burn healing activities.

*Corresponding Author:

Noor Adel Hussein

Email: nooraadi19@gmail.com

Tel.: +009652806704

Introduction

Azo compounds have various applications and noticeable activities; it is the most utilizing dyes [1]. They are used to die many substances, they are a highly colored class of chemical compounds that have been used as dyes and pigments for a long time, and they are attracting interest in scientific research, especially fabrics [2]. The synthesized azo compounds exhibited antimicrobial activity [3], anticancer properties with no toxicity to normal cells, and antifungal activity [4]. Because of their low toxicity, such as hyperactivity and allergic effects, most azo-dyes are used in food, pharmaceuticals, paint, polymers, and standard materials [5]. A large number of researches on the synthesis and conformational characteristics of azo compounds have been conducted in recent years [6]. A lot of work on the azo compound exploits the existence of the bridge azo (- N = N-) group to create novel compounds containing transition metal ions [7]. The novel approaches were used to generate more effective and specific target medications, which has sparked interest among inorganic chemists in new azo dye investigations [8]. Caffeine is the most extensively used behaviorally active drug on the planet [9,10], and changes in glucose metabolism are linked to it [11].

Caffeine is found in a variety of over-the-counter analgesics. Caffeine has several drug-drug and drug-food interactions that are well-known and well-documented. Caffeine's propensity to form complexes with these pharmacological molecules is thought to be responsible for some of these interactions [12]. Some antibacterial drugs' inhibitory effects have been reported to be affected by methyl xanthine in general [13]. There is a

well-documented interaction between caffeine-containing foods and antibacterial drugs [14]. The presence of an azo moiety (-N=N-) that connects two sp2 hybridized carbon atoms, and these carbons are frequently part of an extensive delocalized electron system involving the aromatic ring, identifies them [15]. This article focuses on the synthesis and spectral identification for novel ligand (SNAC) and its complexes with [[Ag(I), Co(II), Cu(II), Pd(II), and Pt(IV)] and study the biological, anticancer and burn healing activities.

Experimental

Instruments and materials

All of the materials and solvents used were of the greatest quality possible. The ligand and its complexes have their elemental analyses and metal content assessed using (C.H.N.S) (Eure EA 3000 Elemental analyzer). pH meter JENWAY 3020 FT-IR spectrophotometry is a type of spectrophotometry that uses infrared Transform of the Fourier Series. The SHIMADZU 8400s spectrophotometer was used to record infrared spectra in the range

(250- 4000) cm^{-1} with CsI. The (SHIMADZU 1800 – UV-Vis spectrophotometer) was used to record UV-Vis spectra for all of the substances examined in the range of (250-1100) nm. On a BRUKER AV 400 Avance -III, the 1H-NMR spectra were measured (400 MHz and 100 MHz). The metal content of the produced ligands and complexes was evaluated by thermal analysis (TGA and DSC) (SDT Q600 V20.9 Build). Gallenkamps melting point device was used to determine the melting points of all the compounds. Indeionized distilled water (10^{-3} M), the molar conductance of metal ion complexes was investigated. The Mohr method was used to determine the chloride content of the investigated complexes. The magnetic susceptibility of the investigated complexes was measured at room temperature using a Sherwood Scientific Auto Magnetic Susceptibility Balance Model.

Synthesis of 8-[5-(2 sulfonic acid naphthyl)azo] Caffeine(SNAC)

This ligand was synthesized using a method described in the literature [16] with a few tweaks as shown in Scheme 1.
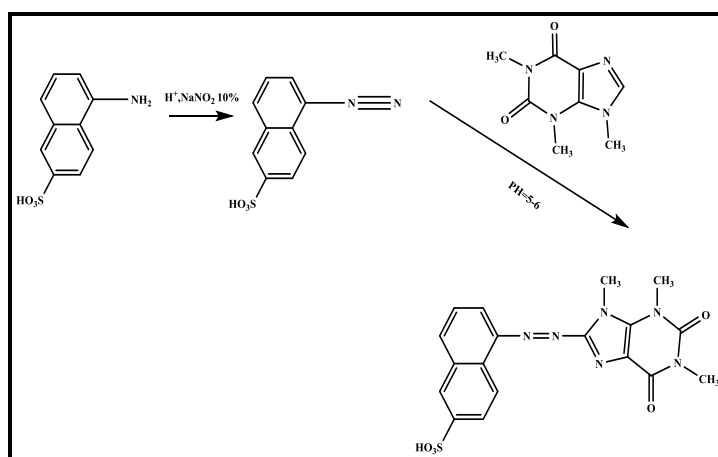
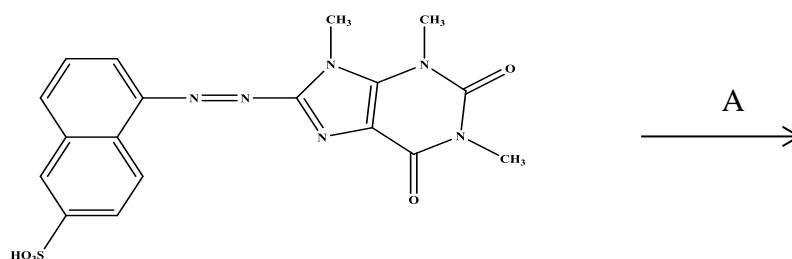**SCHEME 1** Synthesis of SNAC ligand

The diazonium chloride solution was made by dissolving 0.01 mole (2.23 gm) of 5-amino-2-naphthalene sulfonic acid in an ice acidic medium (30 mL distilled water, and 14 mL conc. HCl). The sodium nitrite (0.83 gm

$NaNO_2$) was carefully and dropwise added to the 25 mL water (0 °C). The diazotation was then completed by stirring the diazonium salt for 30 minutes.

The resultant diazonium salt solution was added into a (0.01 mole;1.94 gm) solution of Caffeine in [14 mL ,10% KOH ethanolic]with cooling and stirring. The pH was adjusted to a neutral value (pH = 5-6), and the complexes were synthesized overnight to ensure complete precipitation, filtered and rinsed with (1:1) (ethanol:H$_2$O) to eliminate any residue of the starting material before drying.
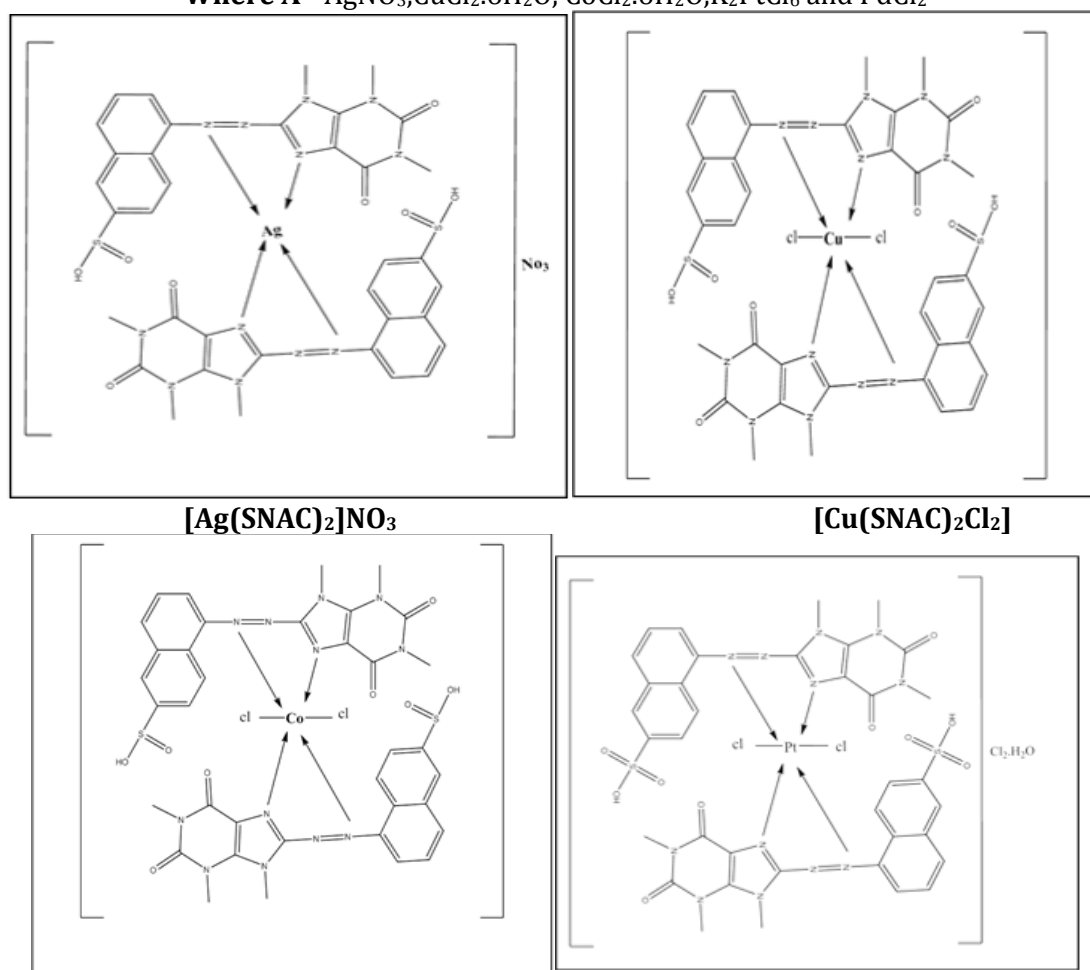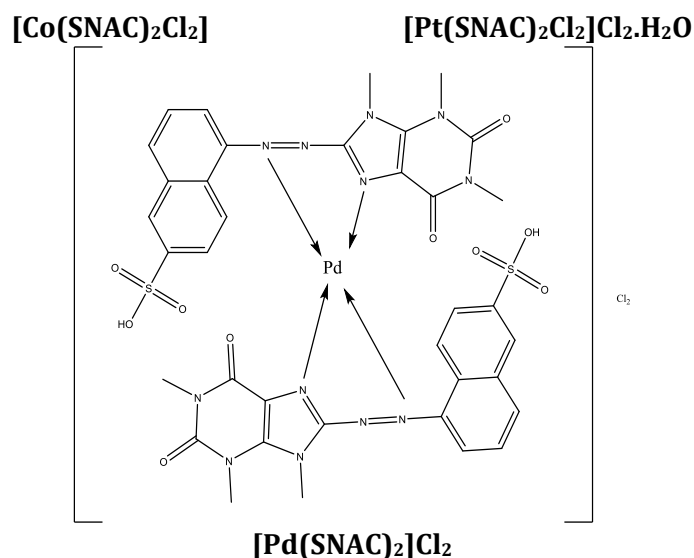
Synthesis of complexes

All complexes were made at a mole ratio (M:L) of 1:2 by dissolving (2 mmole; 0.856 gm) of the ligand SNAC in the smallest amount ofdeionized distilled water possible. The ligand solution was slowly added to the metal salts solution [AgNO$_3$, CuCl$_2$.6H$_2$O, CoCl$_2$.6H2O, K$_2$PtCl$_6$ and PdCl$_2$], which contained an exact amount of each metal salt dissolved in water. For 3 hours, the mixture was reflexed. TLC technical (Scheme 2) was used to monitor the reaction.

SCHEME 2 Synthesis of complexes

Where A= AgNO$_3$,CuCl$_2$.6H$_2$O, CoCl$_2$.6H$_2$O,K$_2$PtCl$_6$ and PdCl$_2$

[Ag(SNAC)$_2$]NO$_3$

[Cu(SNAC)$_2$Cl$_2$]

P a g e | 70

SAMI

Eurasian
Chemical
Communications

N.A. Hussein and A.K. Abbas

[Co(SNAC)₂Cl₂]   **[Pt(SNAC)₂Cl₂]Cl₂.H₂O**

[Pd(SNAC)₂]Cl₂

Antibacterial for the ligand SNAC and its complex

One type of gram-negative bacteria, Escherichia coli (E-Coli), and one type of gram-positive bacteria, Staphylococcus aureus, were examined in this study. The microorganisms were cultivated on a nutritional agar medium for use in this investigation, and the ligand (SNAC) and its complex were dissolved in distilled water. The disc method was used to check the biological inhibition agent of the isolated bacteria for the ligand (SNAC) and its complex. The disc was filled with (5 mm) of $(1 \times 10^{-3}$ M) of the given ligands and their complexes, then left for about 15 minutes before being published on the medium and incubated at 37 °C for 24 hours. For this determination, the consumption diameters were measured using a defined scale.

Dying manner

The dyeing capabilities of the ligand (SNAC) and its complex, which were applied to a wool fabric, are dependent on textile colouring foundations and procedures [17](0.2 gm) of azo dyes. The SNAC ligand and its complexes were dissolved in an ethanolic solution of 10% NaOH, then 50 mL ofdeionized distilled water was added. After that, a piece of a clean wool fabri (10×10) cm,

(30 gm $\pm$ 3 gm) that soaked indeionized distilled water for (30) minutes was transferred to the azo dye solution and heated to 60 °C for 10 minutes. The soaked wool piece was washed three times with (250) mLdeionized distilled water containing 1 gm of soap to remove any non-reacting species. Finally dyed raw was dried by hot steam.

Assessment of anti-oxidant activity in vitro

Method

The method described in the literature [18] was adopted to evaluate the reductive ability, in which 1 mL of each concentration of the [Pt(HBAC)₂Cl₂]Cl₂.H₂O and [Pd(SNAC)₂]Cl₂ (0.02, 0.04, 0.08, 0.16, 0.32, and 0.64 mg/ mL) were combined with 1 mL of 0.2 M phosphate buffer (pH 6.6) and 1.5 mL of 1 percent potassium ferri cyanide and incubated for 20 minutes at 50 °C. To stop the process, 1 mL of 10% trichloroacetic acid was added to the liquid. 2.5 mL of the supernatant was combined with 2 mL ofdeionized distilled water and 0.5 mL of freshly made 1 percent Ferric chloride after centrifugation for 10 minutes at 3000 rpm. The absorbance was then measured at 700 nm. The Trolox solutions were treated in the same way (standards). All of the tests were carried out in duplicate.

DPPH radical scavenging activity

Based on the radical scavenging action of the stable DPPH free radical, the antioxidant activity of $[Pd(SNAC)_2]Cl_2$ and standard (vitamin C) was determined using the method described in the literature [19]. In a test tube, an aliquot of 0.1 mL extract or standard (0.625, 0.125, 0.250, and 0.500 mg/mL) was added to 3.9 mL DPPH solution. The absorbance of each solution was measured at 517 nm using a spectrophotometer after 30 minutes of incubation at 37 °C. Triplicates of all measurements were taken. The following equation was used to calculate the ability to scavenge DPPH radicals:

$$\text{DPPH radical scavenging activity}\,(\%)=\left(1-\frac{\text{Absorbance of Sample}}{\text{Absorbance of Standard}}\right)\times100$$

Anticancer activity

Using the MTT ready to use kit, the cytotoxic effect of different concentrations (6.2, 12.5, 25, 50, 100, 200, and 400 g/mL) of $[Cu(SNAC)_2Cl_2]$ loaded on S. official was investigated.

• Tumor cells ($1x10^4$–$1x10^6$ cells/mL) were cultured on 96 flat well micro-titer plates with a final volume of 200 L complete culture media per well. The microplate was wrapped with sterilized parafilm and gently shacked.

• Plates were incubated for 24 hours at 37 °C with 5% CO_2.

• After removing the medium, successive dilutions of the required concentrations of $[Cu(SNAC)_2Cl_2]$ (6.2, 12.5, 25, 50, 100, 200, and 400 μg/mL) was added to the wells.

• For each concentration and the controls, triplicates were employed (cells treated with serum free medium). Plates were incubated at 37 °C with 5% CO_2 for the duration of the exposure time (24 hours).

• In each well, 10 l of MTT solution was added. Plates were then incubated for another 4 hours at 37 °C with 5% CO_2.

• After incubation, the media were carefully removed, and each well received 100 mL of solubilization solution for 5 minutes.

Using an ELISA reader to measure at a wavelength of 575 nm, statistical analysis of optical density data was used to determine the concentration of chemicals required to cause a 50% drop in cell viability for each cell line [20].

Results and discussion

The synthetic path for the ligand (SNAC) was depicted in Scheme 1, which was synthesized by the diazotization of [5-(2-sulfonic acid naphthyl)] at (0-5) °C to keep the diazonium salt formed from disintegration. Then it is coupled with an ethanolic alkaline solution of caffeine as a nucleophile. Reacting the organized ligand (SNAC) with a selection metal ions [Ag(I), Co(II), Cu(II), Pd(II), and Pt(IV)] with the mole ratio [M:L][1:2], the ligand acts as neutral N,N-bidentate. The consequences and physical features were gotten from [C.H.N], metal content and chloride ion by Mohr method for the organized compounds which are listed in Table 1 and in good agreement with those required by the suggested formulae. Also, the formulae of the synthesized compound were suggested depending on the information obtained from spectral studies, magnetic susceptibility, and molar conductivity. The ligand and its complexes had color pink, brown, and red. They are all soluble in the water.

TABLE 1 Physical characteristics and elemental analyses

Compounds (M.wt)(gm/mol)	M:L	Color λ (nm)	%Experimental (Theoretical)%				
			C%	H%	N%	Cl%	M
SNAC($C_{18}H_{16}N_6O_5S$) 428	1:2	light pink 505	51.86 (50.46)	3.763 (3.73)	20.05 (19.62)	---	---
[Ag($C_{36}H_{32}N_{12}O_{10}S_2$]NO$_3$ 1035.88	1:2	reddish pink 548	43.31 (42.11)	3.99 (3.11)	17.30 (17.7)	10.22 (10.51)	---
[Cu($C_{36}H_{32}N_{12}O_{10}S_2$)Cl$_2$] 990.54	1:2	pink 515	43.27 (43.61)	4.05 (3.23)	16.92 (16.96)	5.48 (6.41)	7.14% (7.16)%
[Co($C_{36}H_{32}N_{12}O_{10}S_2$)Cl$_2$] 985.93	1:2	greenish brown 573	43.22 (43.81)	3.62 (3.24)	17.98 (17.03)	5.51 (5.92)	7.23% (7.20)%
[Pt($C_{36}H_{32}N_{12}O_{10}S_2$)Cl$_2$]Cl$_2$.H$_2$O 1132.88	1:2	green 623	38.77 (38.13)	3.67 (3.00)	15.08 14.82)	17.11 (17.21)	12.36% (12.53)%
[Pd($C_{36}H_{32}N_{12}O_{10}S_2$)]Cl$_2$ 1034.42	1:2	green 627	41.26 (41.8)	3.42 (3.11)	17.14 (16.25)	9.97 (10.28)	6.49 (6.81)%

Proposition the mole ratio

The mole ratio approach, which is the most widely used method for determining the composition of a complex in solution, was used [21]. The result indicates that the formation of [1:2][M:L] all created complexes have a mole ratio (Table 2 and Figure 1).

TABLE 2 The Absorbance for method of mole ratio of (M-SNAC) solutions at (10^{-3}M)

M:L	Absorbance(λmax)nm for SNAC Complexes at 10^{-3} M				
	Ag-SNAC (548 nm)	Cu-SNAC (515 nm)	Co-SNAC (573 nm)	Pt-SNAC (623 nm)	Pd-SNAC (627 nm)
1:025	0.02	0.21	0.125	0.25	0.55
1:0.50	0.18	0.44	0.191	0.4	0.73
1:0.75	0.52	0.93	0.256	0.71	0.88
1:1	0.75	1.11	0.335	0.89	1.11
1:1.25	0.93	1.27	0.425	1.19	1.3
1:1.50	1.11	1.36	0.515	1.28	1.45
1:1.75	1.25	1.45	0.625	1.49	1.55
1:2	1.27	1.51	0.732	1.51	1.61
1:2.25	1.3	1.53	0.731	1.56	1.62
1:2.50	1.33	1.52	0.733	1.58	1.65
1:2.75	1.39	1.54	0.728	1.61	1.66
1:3	1.4	1.501	0.729	1.6	1.64
1:3.25	1.44	1.55	0.725	1.61	1.65
1:3.50	1.44	1.54	0.726	1.59	1.62
1:375	1.45	1.56	0.732	1.58	1.63
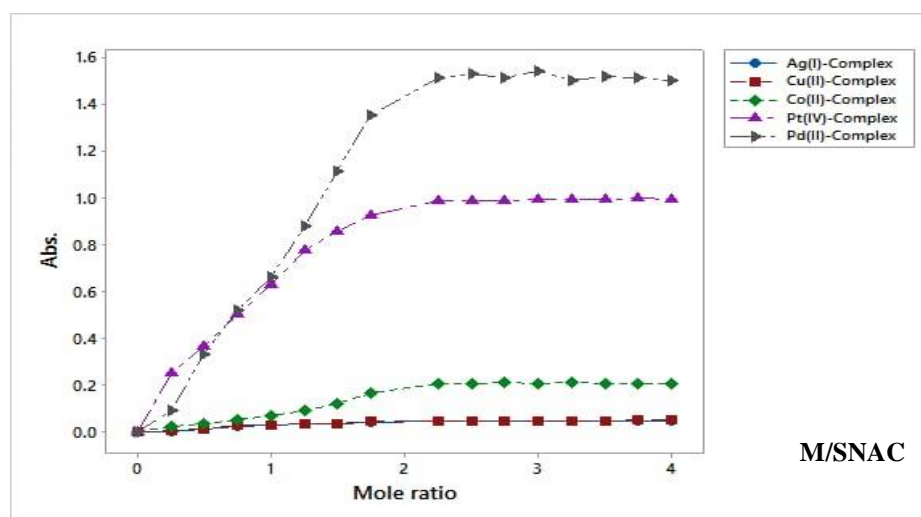
FIGURE 1 Mole ratio plot for [M/SNAC] complex solutions at[10^{-3}M]

Complexes' stability constant and Gibbs free energy

From the equation below, the stability constant (K) for Pt(IV), Co(II), Cu(II), Ag(I), and Pd(II) complexes has been derived [22].

$$K = \frac{1-\alpha}{4\alpha^3 C^2} \; ; \; \alpha = \frac{A_m - A_s}{A_m}$$

Where:

α = The fraction of a mole for the reactant that submits dissociation calling the degree of dissociation.

As = The absorption of a stoichiometric amount of ligand and metal ion in a complex solution.

Am = The absorption of a solution containing a ligand excess.

C = The mole/L concentration of the synthesized solution.

The high K values could be due to the produced compounds' great stability [23]. Table 3 lists all stability constant values for the synthesized complexes, demonstrating that the thermodynamic parameters of Gibbs free energy (ΔG) were computed using the equation [24].

ΔG = -R T ln K

Where:

T = (298 °C) Absolute temperature in Kelvin

R = gas constant = 8.314 J.mol^{-1}.K.

Stability of complexes was increased as follows:

[Cu(SNAC)$_2$Cl$_2$]> [Pd(SNAC)$_2$]Cl$_2$> [Ag(SNAC)$_2$]NO$_3$>[Pt(SNAC)$_2$Cl$_2$]Cl$_2$.H$_2$O> [Co(SNAC)$_2$Cl$_2$]> .
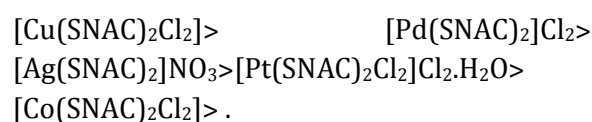
TABLE 3 The Gibbs free energy (G) and the stability constant (K) for the complexes

Complexes	A_S	A_m	α	K	LnK	ΔG
[Ag(SNAC)$_2$]NO$_3$	0.75	1.27	0.409	2159521.666	14.585	-6639.877
[Cu(SNAC)$_2$Cl$_2$]	1.11	1.51	0.264	10000139.13	16.118	-6887.493
[Co(SNAC)$_2$Cl$_2$]	0.33	0.73	0.547	691952.4186	13.44	-6437.315
[Pt(SNAC)$_2$Cl$_2$]Cl$_2$.H$_2$O	0.89	1.51	0.410	2140131.455	14.57	-6494.626
[Pd(SNAC)$_2$]Cl$_2$	1.11	1.61	0.310	5790339.364	15.57	-6654.687

Thermogravimetric analysis (TGA)

The ligand's thermal degradation (SNAC) and its complexes were investigated by (TGA) and from (25-1000) °C in argon. The thermal analysis was performed to prove the proposed formula and study the thermal stability of the synthesized ligand SNAC with its complexes. Furthermore, the peak of the loss for water molecules is predestined from the [Pt(SNAC)Cl$_2$]Cl$_2$.2H$_2$O complexes as alattice water in the step 1 at the ranges (25-
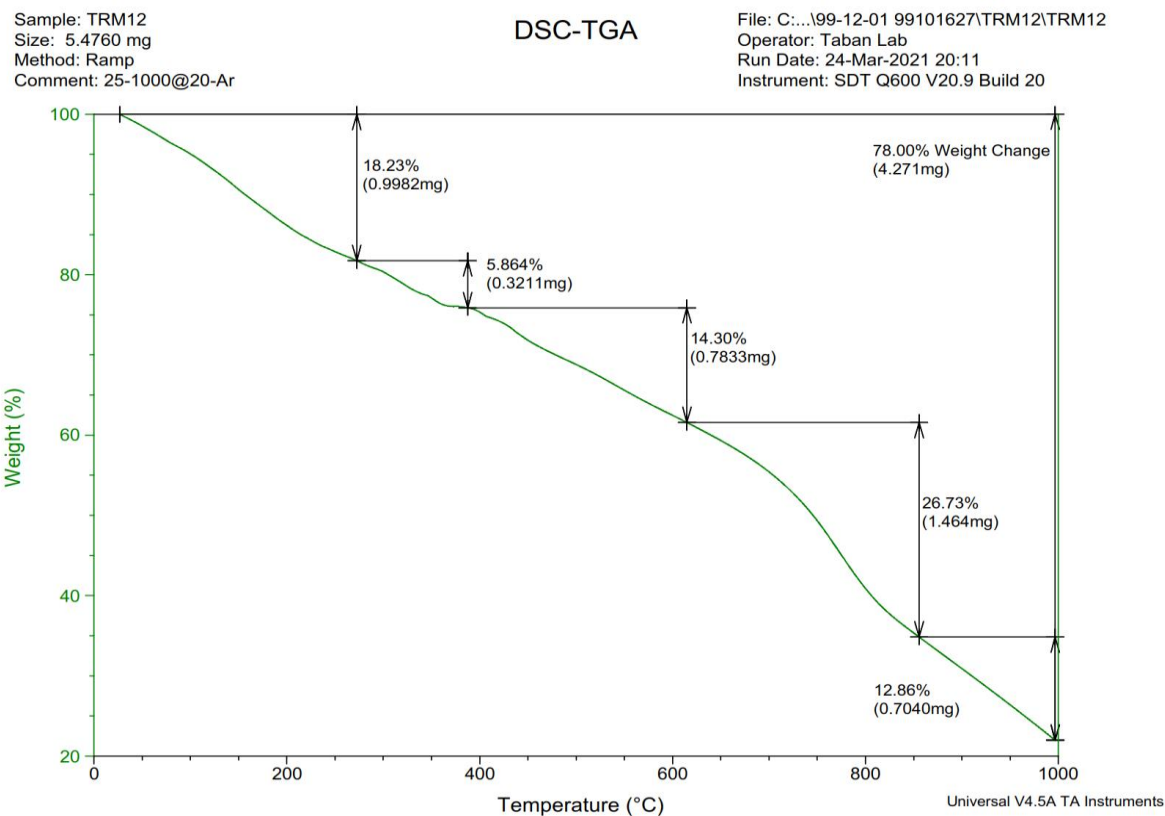
200) °C, thuse the loss of coordinated water can occur over this temperature [25]. The results appear in agood agreement with the formulae suggested from the analytical data [26]. The residue of SCAN is (22%), the thermal stability order of the number of SNAC complexes is reduced in the following order: $[Pt(SNAC)_2Cl_2]Cl_2.H_2O>$ $[Pd(SNAC)_2]Cl_2$ > $[Ag(SNAC)_2]NO_3$ > $[Co(SNAC)_2Cl_2]>$ $[Cu(SNAC)_2Cl_2]$ (51.7%) (42%) (30%) (27.3%) (15.47%)

TABLE 4 TGA of ligand (SNAC) and its complexes

| Com. Sym	Molecular Formula (molecular Weight) g/mole	Steps	TG. Range of the decomposit i on (°C)	Suggested Assignmen t	Mass loss%	
					Calculate %	Found %
SNAC	$C_{18}H_{16}N_6O_5S$ 428 gm/mole	1	275-400 °C	C_6H_6	18.22%	18.23%
		2	395-400 °C	C_2H	5.84%	5.86%
		3	600 °C	C_5H	14.25%	14.30%
		4	850-1000 °C	$C_5H_8N_2O$	26.16%	26.73%
		5	1000 °C	N_4	13.08%	12.86%
		Residue	>1000 °C	O_4S	22.4%	22%
[Ag(SNAC)₂]NO₃	$C_{36}H_{32}N_{13}O_{13}S_2Ag$ 1025.86 gm/mole	1	400-500 °C	$C_{11}H_{11}$	13.9%	14%
		2	500-600 °C	C_5H_{12}	7%	7%
		3	600-700 °C	C_8H_6	9.9%	10%
		4	800-900 °C	$C_{12}H3N_{13}O_{4.5}$	39%	39%
		Residue	>1000 °C	$O_{8.5}S_2Ag$	30%	30%
[Cu(SNAC)₂Cl₂]	$C_{36}H_{32}N_{12}O_{10}S_2CuCl_2$ 990.54 gm/mole	1	80-200 °C	$Cl_2C_6H_7$	15.14%	15.15%
		2	225-400 °C	C_8H_{11}	10.80%	10.88%
		3	350-400 °C	$C_{14}N_7$	26.85%	26.91%
		4	610-800 °C	$C_8H_{11}N_5$	17.86%	17.95%
		5	1000 °C	$H_3O_7S_{0.6}$	13.58%	13.64%
		Residue	1000 °C>	$S_{1.4}CuO_3$	15.78%	15.47%
[Co(SNAC)₂Cl₂]	$C_{36}H_{32}N_{12}O_{10}S_2CoCl_2$ 985.93 gm/mole	1	150-200 °C	Cl_2C_5	13.28%	13.20%
		2	265-400 °C	C_9H_4	11.35%	11.40%
		3	480-600 °C	$C_{14}H_7$	17.74%	17.75%
		4	830-1000 °C	$C_8H_4 N_5$	17.24%	17.24%
		5	1000 °C	$H_{14} N_7O$	12.98%	13.08%
		Residue	>1000 °C	$H_3O_9S_2Co$	27.3%	27.3%
[Pt(SNAC)₂Cl₂]Cl₂.H₂O	$C_{36}H_{34}N_{12}O_6S_2Cl_4Pt$ 1132.88 gm/mole	1	25-200 °C	C_2H_4O	3.88%	3.69%
		2	425-600 °C	$C_4H_{11}Cl_4$	17.74%	17.75%
		3	870-1000 °C	$C_{19}H_3N$	21.13%	21.50%
		Residue	>1000 °C	$PtC_{11}N_{11}H_{16}O_5S_2$	50.12%	51.7%
[Pd(SNAC)₂]Cl₂	$C_{36}H_{32}N_{12}O_{10}S_2PdCl_2$ 1034.42 gm/mole	1	300-400 °C	C_9H_{15}	11.89%	12%
		2	400-550 °C	$Cl_2C_{16}H_5$	25.9%	26%
		3	800-900 °C	C_6H_{10}	7.9%	%8
		4	900-1000 °C	$C_5H_2N_{4.5}$	12%	12%
		Residue	>1000 °C	$N_{7.5}O_{10}S_2Pd$	42%	42%

FIGURE 2 TGA for the (SNAC) ligand
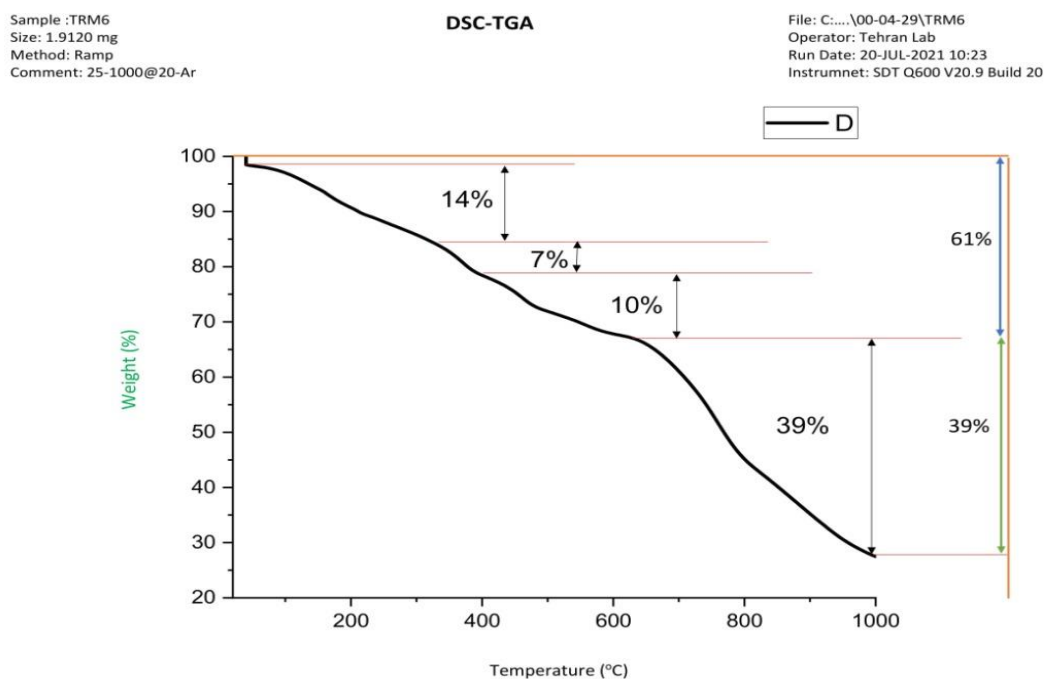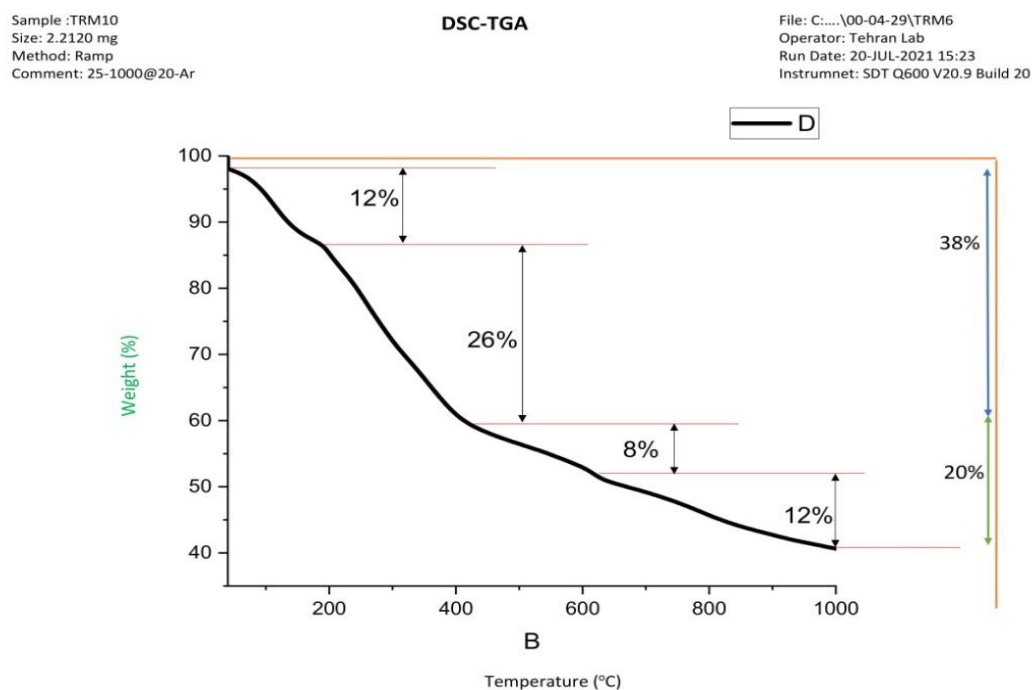

FIGURE 3 TGA for the [Ag(SNAC)$_2$]NO$_3$ complex
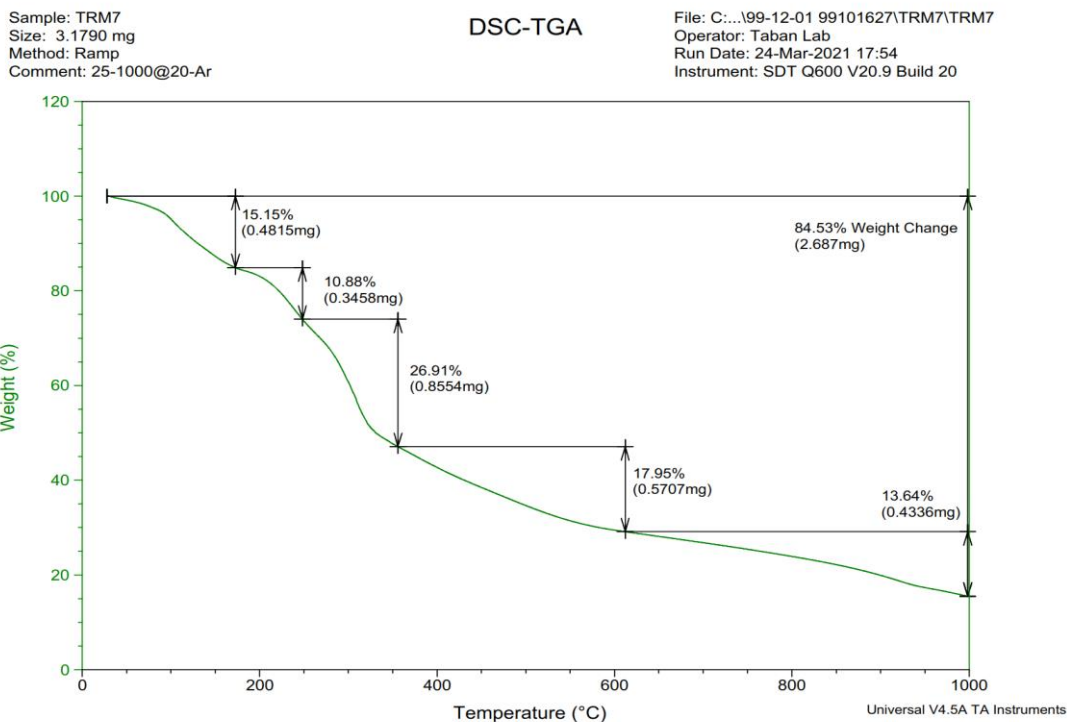
FIGURE 4 TGA for the [Cu(SNAC)$_2$Cl$_2$] complex
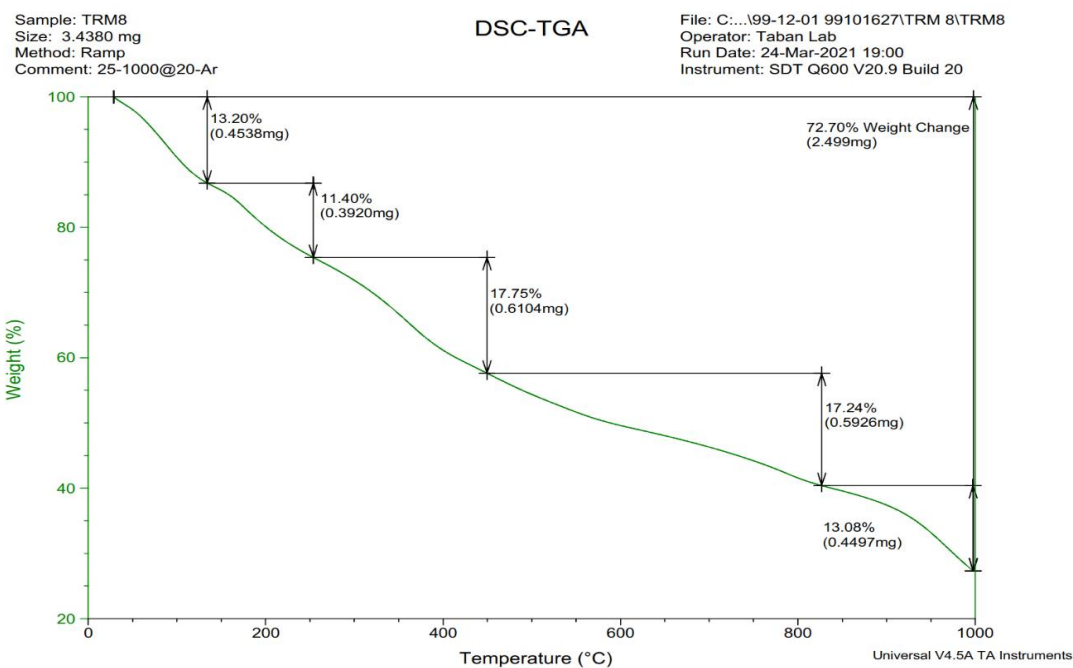
FIGURE 5 TGA for the [Co(SNAC)$_2$Cl$_2$] complex
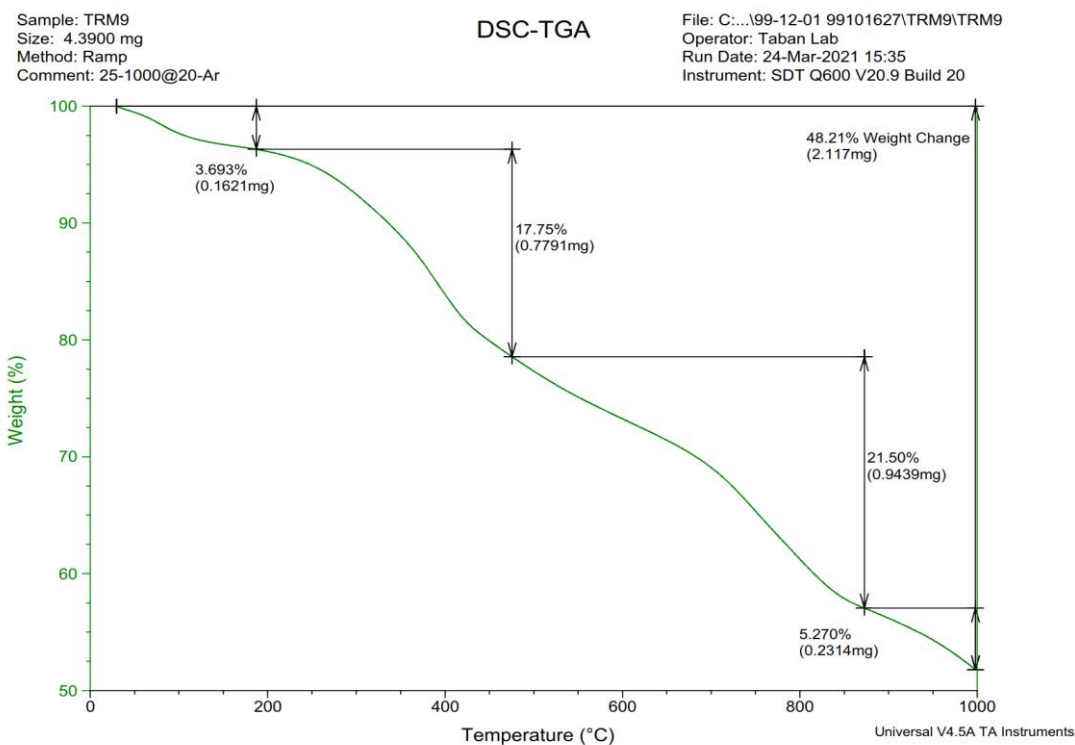
FIGURE 6 TGA for the [Pt(SNAC)$_2$Cl$_2$]Cl$_2$.H$_2$O complex

FIGURE 7 TGA for the [Pd(SNAC)$_2$]Cl$_2$ complex

UV-Vis spectral studies

The colored containe reaction of metal ions with azo ligands is very important for electronic spectral studies. Electronic spectral properties focus on differences between the ground state and excited state of molecule [27]. The electronic spectra for the

ligand(SNAC) and its complexes were measured (10^{-4} M) in deionized distilled water within the range (200-1100) nm at room temperature.

The electronic spectra for the ligand (SNAC) display two-band, the first at (505 nm, 19801 cm-1), while the second at (398 nm; 25125 cm-1). The first band was attributed a moderate amount of energy (n→ π^*) transition of the intra molecular charge transfer (intra CT) taken place *via* carbonyl and azo moieties. The second band in the UV region was reverted to $(n \to \pi^*)$ intermolecular transition [inter CT]for pyrimidine and naphthalene moieties [28].

The electronic spectra for [Pt(SNAC)$_2$Cl$_2$]Cl$_2$.H$_2$O clarified bands at (964 nm; 10373 cm-1) that assigned to [^{1}A$_1$g →^{1}T$_1$g] transition. At the same time, the transition [^{1}A$_1$g →^{1}T$_2$g] was taken at (780 nm, 12820 cm-1). The forbidden transition [^{1}A$_1$g →^{3}T$_1$g] was hidden with (LMCT) transition at (623 nm, 16051 cm-1). This is within octahedral geometry [29] as was shown in Figure 9. The [Cu(SNAC)$_2$Cl$_2$] complex showed two band (Figure 10). The broad bands at (963 nm; 10384 cm-1) related

to [^{2}B$_1$g→^{2}A$_1$g] transition but the band at (515 nm; 19417 cm-1) was attributed to [^{2}B$_1$g→ ^{2}Eg] transitions. The LMCT was merged with [^{2}B$_1$g→ ^{2}Eg] which had distorted octahedral D$_4$h. Three main transitions were usually assigned to the octahedral complexes for Co(II) complexes as it follows:
[v_1= ^{4}T$_1$g$_{(F)}$ → ^{4}T$_2$g$_{(F)}$],[v_2=^{4}T$_1$g$_{(F)}$ → ^{4}A$_2$g$_{(F)}$]and [v_3=^{4}T$_1$g$_{(F)}$ → ^{4}T$_1$g$_{(P)}$].
[Co(SNAC)$_2$Cl$_2$] complex was appeared three transitions at(1065 nm;938 cm-1) v_1, (880 nm; 11363 cm-1)v_2 ,respectively.The(LMCT) transition was noticed at (573 nm; 17452 cm-1) $v_3$as was shown in Figure 11. The complex [Pd(SNAC)$_2$]Cl$_2$ was appeared two transitions only that belong to [^{1}A$_1$g → ^{1}A$_2$g] transition at (917 nm, 10905 cm^{-1}). As for the transition [^{1}A$_1$g→ ^{1}E$_1$g] is so very weak therefore is hidden At the visible range for the spectrum of [Pd(SNAC)$_2$Cl$_2$] a double band at (627nm;15948cm-1)which assigned to (LMCT) and the same band was observed at(627 nm;15948 cm-1) (Figure 12) [30].
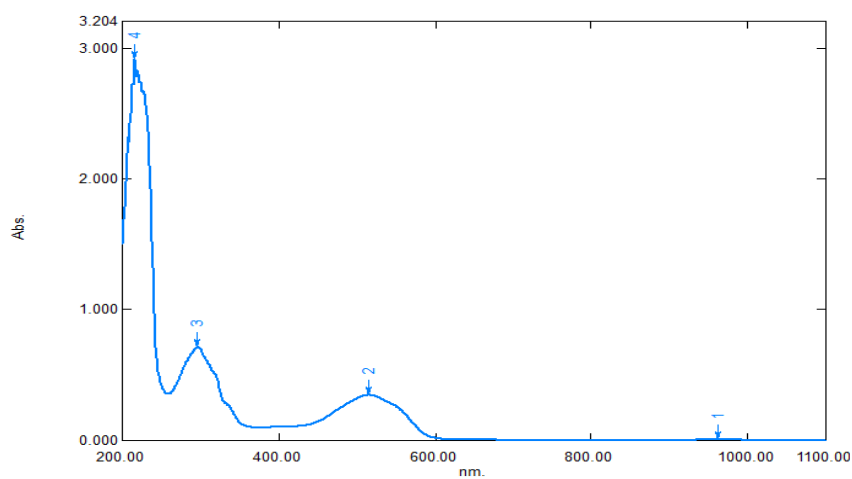
The UV-Vis spectrum for Ag-complex (d^{10}) diamagnetic [Ag(SNAC)$_2$]NO$_3$ showed a sharp absorption band at (548 nm; 18248 cm-1) (Figure 13), which is assigned to transition ($\pi→\pi^*$)(CT) [31].
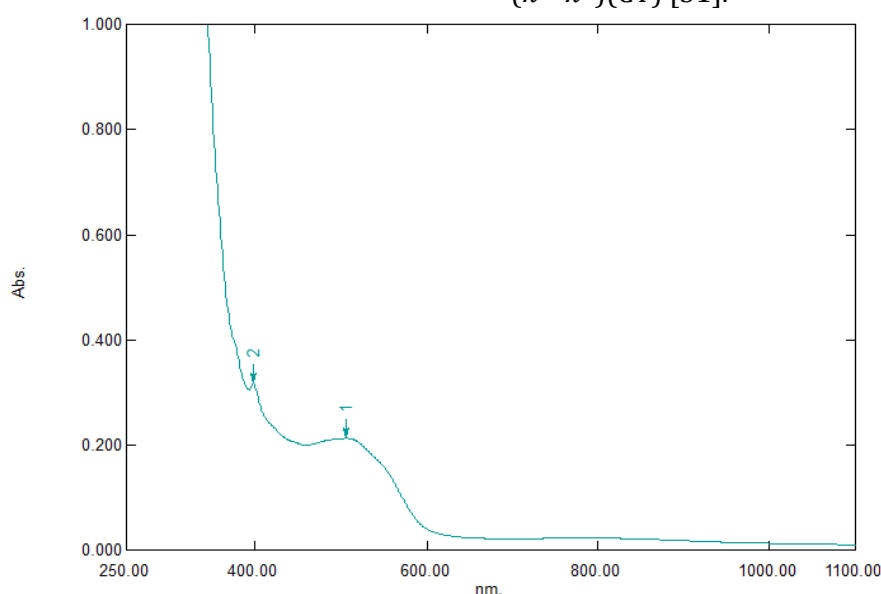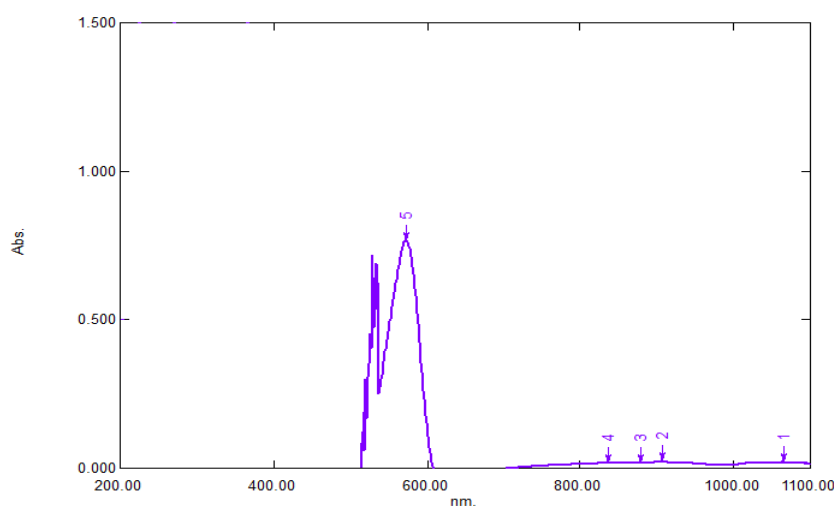
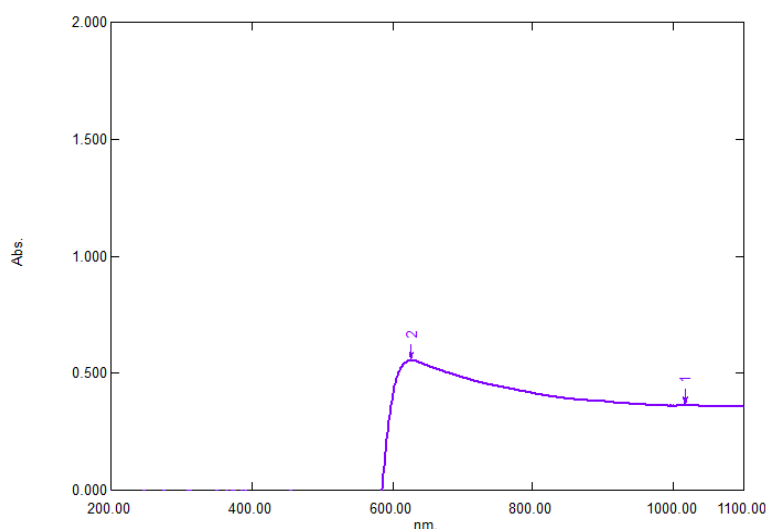

FIGURE 8 The UV-Vis spectrum of the SNAC ligand
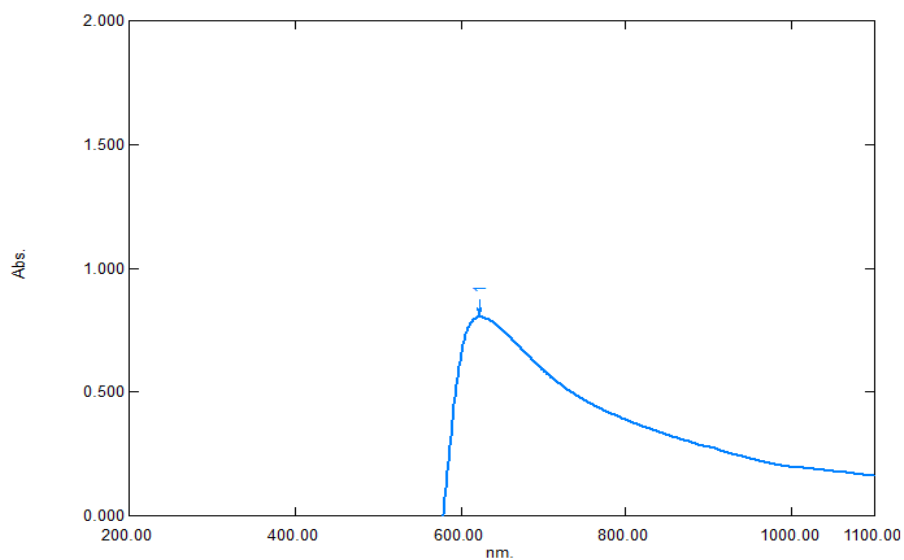
FIGURE 9 The UV-Vis spectrum of the $[Pt(SNAC)_2Cl_2]Cl_2.H_2O$ complex
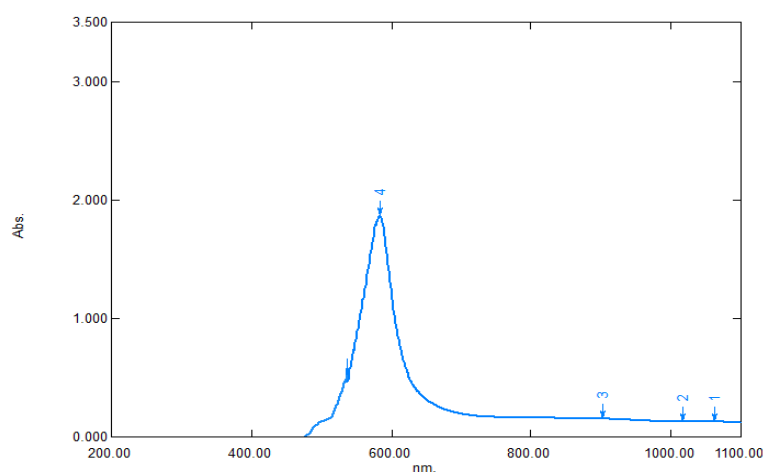

FIGURE 10 The UV-Vis spectrum of the $[Cu(SNAC)_2Cl_2]$ complex

FIGURE 11 The UV-Vis spectrum of the $[Co(SNAC)_2Cl_2]$ complex

FIGURE 12 The UV-Vis spectrum of the $[Pd(SNAC)_2]Cl_2$ complex

FIGURE 13 The UV-Vis spectrum of the $[Ag(SNAC)_2]NO_3$ complex

TABLE 5 Electronic transition, hybridization, and geometry observed at the ligand and its complexes at (10^{-4} M)

| Compound	$\lambda(nm)$	Wave number (cm^{-1})	Assignment	Geometry
SNAC	398	25125	$n \rightarrow \pi^*$	---
	505	19801	$n \rightarrow \pi^*$	
$[Ag(SNAC)_2]NO_3$	548	18248	$n \rightarrow \pi^*$	Tetrahedral
$[Cu(SNAC)_2Cl_2]$	963	10384	$^2B_{1g} \rightarrow {}^2A_{1g}$	Tetragonal
	515	19417	CT	
$[Co(SNAC)_2Cl_2]$	1065	9389	$^4T_{1g(F)} \rightarrow {}^4T_{2g(F)}$	Octahedral
	880	11363	$^4T_{1g\ (F)} \rightarrow {}^4A_{2g\ (F)}$	
	573	17452	CT	
$[Pt(SNAC)_2Cl_2]Cl_2.H_2O$	964	10373	$^1A_{1g} \rightarrow {}^1T_{1g}$	Octahedral
	780	12820	$A_{1g} \rightarrow {}^1T_{2g}{}^1$	
	623	16051	CT	
$[Pd(SNAC)_2]Cl_2$	917	10905	$[^1A_{1g} \rightarrow {}^1A_{2g}]$	Square planar
	627	15948	CT	

1HNMR spectra

The ^{1}HNMR spectra of the synthesized complexes in comparison with the free ligands using TMS as an internal standard include data on chemical shift (δ) in ppm for various types of protons. All results are reported in Table 6; the ^{1}HNMR spectra were recorded in DMSO-d6 solution.

The free ligand (SNAC) displays two singlet signals at (4.1 and 8.81) ppm due to the protons of ($N-CH_{3imd}$) prm and (SO_3H) respectively. Multi signals are appeared at $\delta[[8.15-7.73]]$ ppm for the aromatic ring and naphthalene ring in the spectra of ligand (SNAC. These signals were suffered little shift in the spectra of the complexes due to chelating [32].
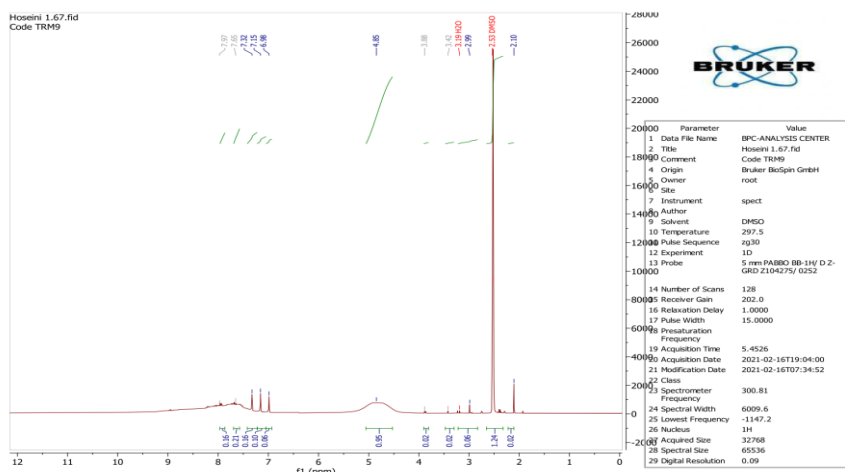
TABLE 6 ^{1}HNMR signals of SNAC and its complexes

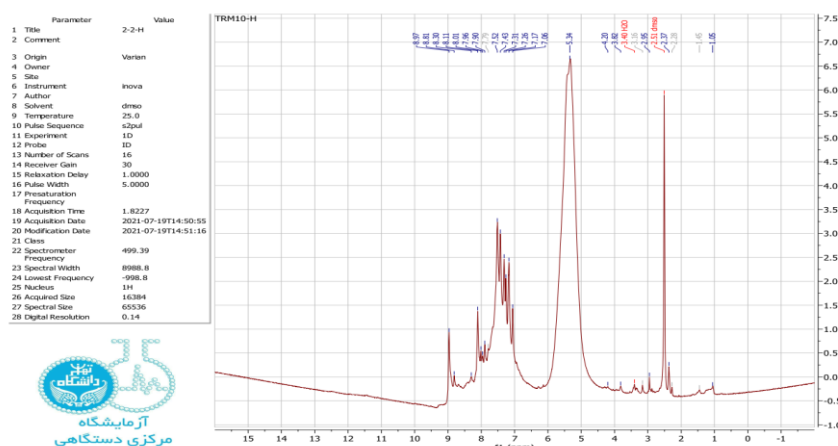| Compound	SO_3H	Ar-H	Naph-H	$N-CH_{3\ imd.}$	$N-CH_{3Pyrm}$
SNAC	8.81	7.77	8.15-7.73	4.1	3.80, 3.4
$[Ag(SNAC)_2]NO_3$	7.67	7.58	8.12	3.35	3.72
$[Pt(SNAC)_2]Cl_2.H_2O$	8.5	7.97	7.65	4.85	3.80, 3.20
$[Pd(SNAC)_2]Cl_2$	8.11	7.96	7.79	4.20	3.24, 3.8
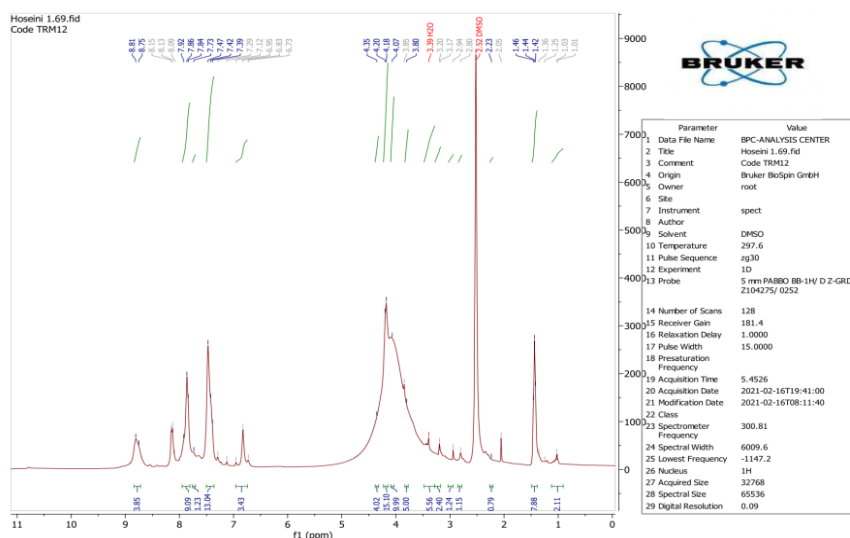
FIGURE 14 ^{1}HNMR spectrum for the (SNAC) ligand
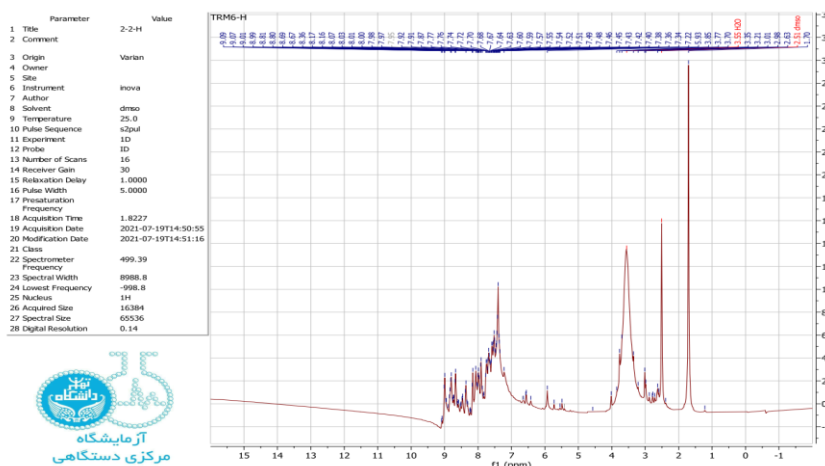
FIGURE 15 ^{1}HNMR spectrum for the $[Ag(SNAC)_2]NO_3$] complex

FIGURE 16 ^{1}HNMR spectrum for the [Pt(SNAC)$_2$Cl$_2$]Cl$_2$.H$_2$O complex

FIGURE 17 ^{1}HNMR spectrum for the [Pd(SNAC)$_2$]Cl$_2$ complex

FTIR spectra

The FT-IR spectra for the ligand (SNAC) were compared with the synthesized metal ions complexes. The spectra of the complexes appeared absorption bands back to the ligand with some differences due to the chelating. The main bands for the ligand (SNAC) and metal complexes are summarized in Table 7, while Figures [18-23] appeared the most moieties vibration which was carried out in the range (250-4000) cm^{-1} using CsI disk.

In the spectra of the ligand (SNAC) a band was (1695) cm^{-1} which related to υ(C=N) in the imidazole ring for the caffeine.This band was altered in position and shape or disappearing due to coordination with metal ion [33]. The characteristic feature bands for the azo compounds are υ (C-N=N-C) and υ(N=N). These bands appeared at (1450) cm^{-1} and (1224) cm^{-1} in spectra for (SNAC) respectively. The position and intensity of these bands were diminished in the complex spectra by complexation [34].

The new bands were appeared in the range (688-659) cm^{-1},(516-549) cm^{-1} and (418-435) cm^{-1} which attributed to υ(M-N)$_{imd}$, υ(N-N)$_{azo}$ and υ (M-Cl) respectively indicating the chelation and the ligand (SNAC) acts as neutral N,N,bidentate.

TABLE 7 Main band of FTIR for the ligand (SNAC) and it complex

Com.	υ(OH)	υ C=O	υ C=N	υ N=N	υ(-C-N=N-C-)	υ(M-N) imd	υ (M-N) azo	υ(M-Cl)
SNAC	----	1695	1618 1653 } m } d	1450 m	1224.	-	-	-
[Ag(SNAC)$_2$]NO$_3$	----	1610 1587	1504	1417 1367 }	1199 st.	688	541	-
[Cu(SNAC)$_2$Cl$_2$]	----	1650w	1593 (vw)	1456 1434 } d	1190 st.	690	518	424
[Co(SNAC)$_2$Cl$_2$]	-----	1585 1625m	1533(vw)	1465 1433 } d	1186 1157 } d .	690	516	435
[Pt(SNAC)$_2$Cl2]Cl$_2$.H$_2$O	3502 3458 3444	1618m	1595(vw)	1452 vw.	1226 1207 } d, st	686	520	420
[Pd(SNAC)$_2$]Cl$_2$	-----	1623w	1596 (vw)	1438vw.	1197 1178 1159 } t. st	688	549	418
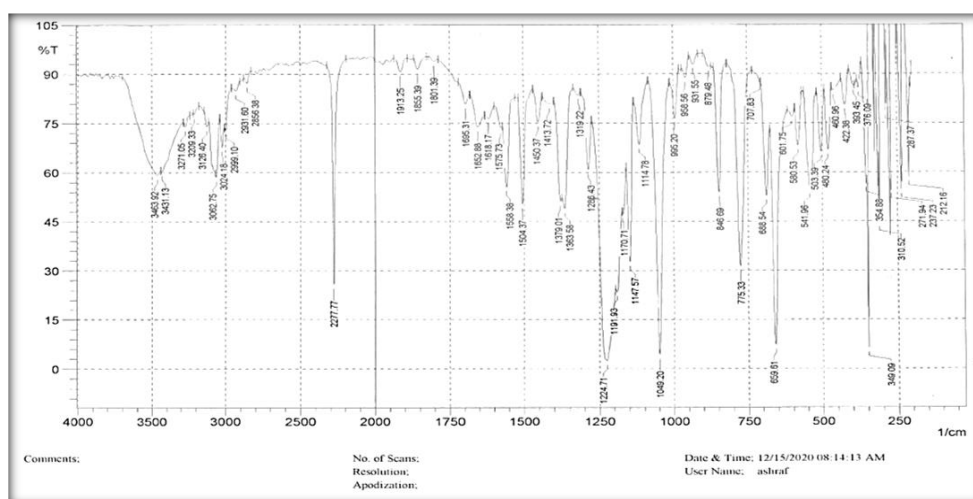
FIGURE 18 FTIR spectrum of SNAC ligand
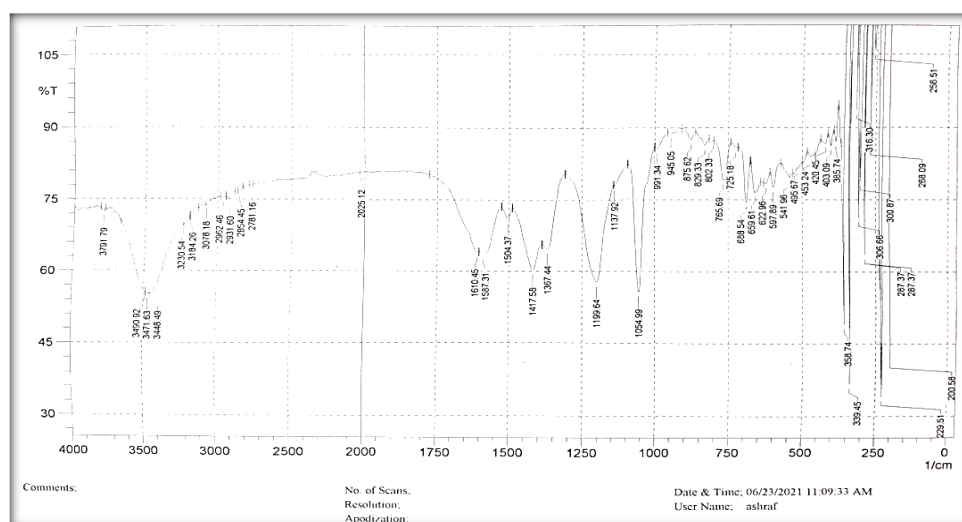
FIGURE 19 FTIR spectrum of [Ag(SNAC)$_2$]NO$_3$ complex

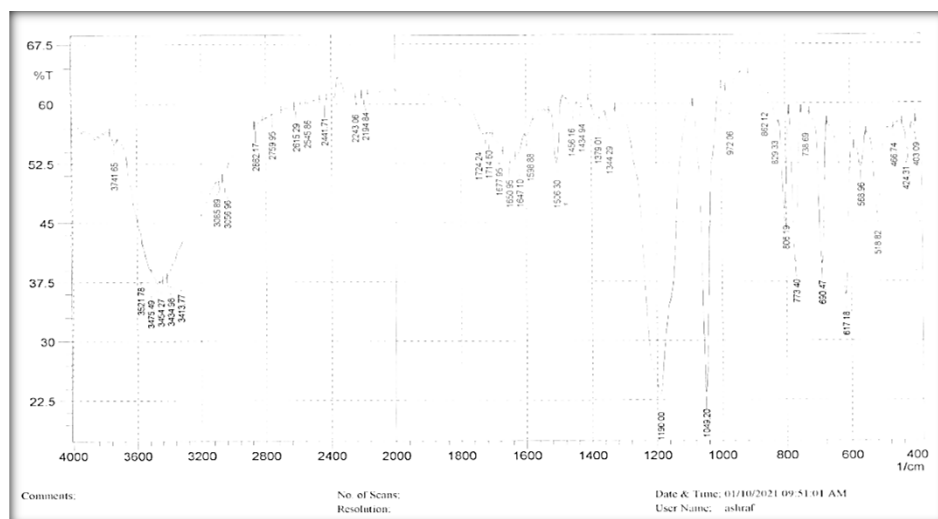**SAMI** Eurasian Chemical Communications

FIGURE 20 FTIR spectrum of [Cu (SNAC)$_2$Cl$_2$] complex
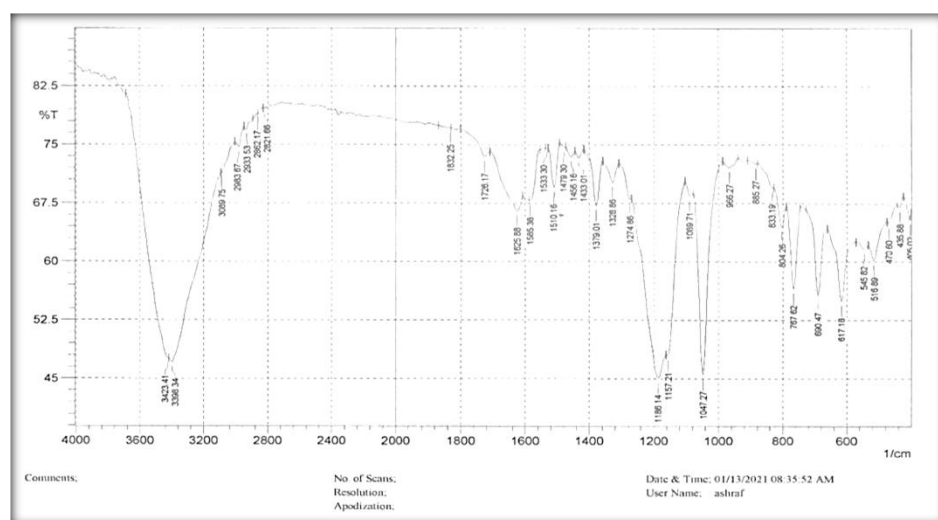
FIGURE 21 FTIR spectrum of [Co(SNAC)$_2$Cl$_2$] complex
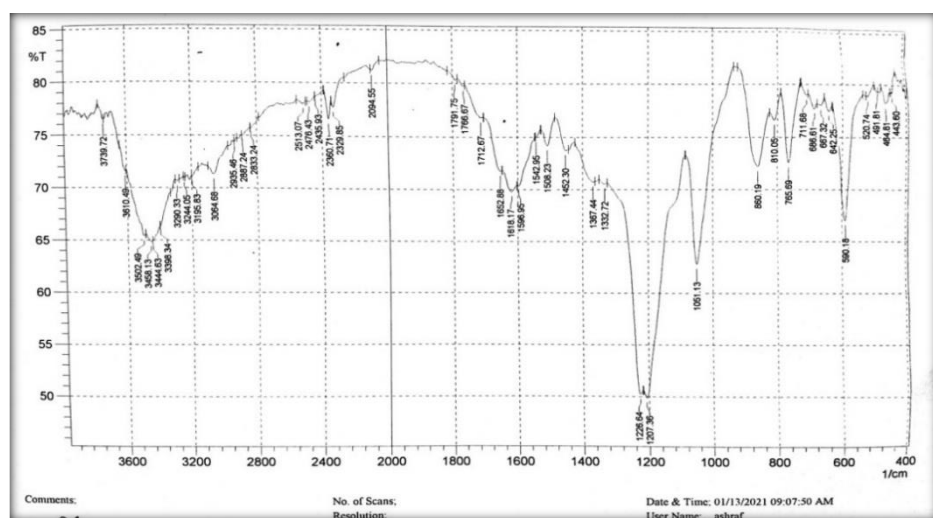
FIGURE 22 FTIR spectrum of [Pt (SNAC)$_2$Cl$_2$]Cl$_2$.H$_2$O complex
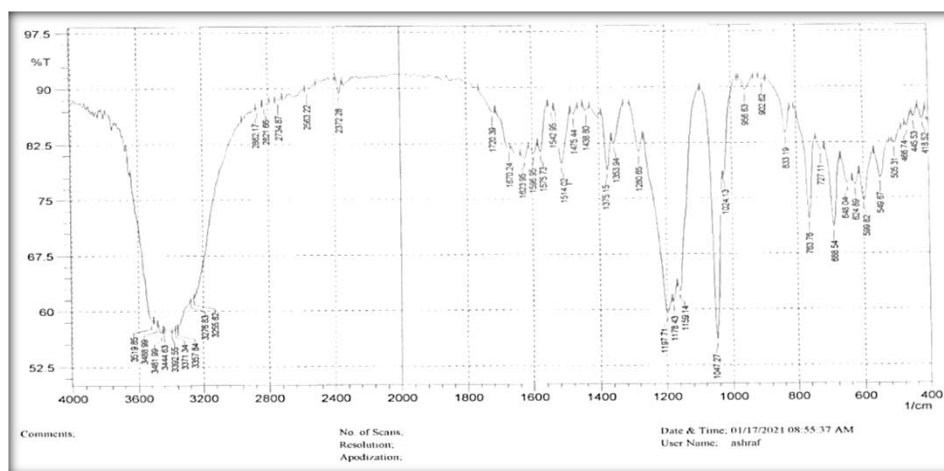
FIGURE 23 FTIR spectrum of [Pd (SNAC)2]Cl$_2$ complex

Magnetic susceptibility

From Table 8, a diamagnetic property was recorded for low spin octahedral (d^6) t$_2$g^{6}eg^0 Pt(IV), tetrahedral (d^{10}) t$_2$g^{6}eg^4 Ag(I), and square planer (d^8) t$_2$g^{6}eg^2 Pd(II) while a para magnetic properties were observed for high spin (d^9)Cu(II) and (d^7)Co(II) complexes. This fits in with the literature regarding of the distorted octahedral complexes for Cu(II) d^9 (t$_2$g^6 eg^3) and Co(II) d^7 (t$_2$g^6 eg^1) [35].

TABLE 8 Magnetic moments of all complexes, theoretical and experimental

Complexes	Theoretical (B.M.)	Experimental (B.M.)
[Ag(SNAC)$_2$]NO$_3$	Dia	Dia
[Cu(SNAC)$_2$Cl$_2$]	1.70	1.8
[Co(SNAC)$_2$Cl$_2$]	3.82	3.86
[Pt(SNAC)$_2$Cl2]Cl$_2$	Dia	Dia
[Pd(SNAC)$_2$]Cl$_2$	Dia	Dia

Molar conductivity measurements

The molar conductance for every synthesized complex was measured in deionized distilled water with (10^{-3} M). The results were depicted in Table 9. The Cu-SNAC, Co-SNAC and Pd-SNAC are non-electrolyte properties. As Ag-complexes with the two ligands have (1:1) electrolyte properties with nitrate as a counter ion while, Pt-complexes have (1:2) electrolyte properties and the chloride ion as a counter ion.

TABLE 9 Molar conductance of synthesized complexes in deionized distilled water solvent

Compounds	Λm (S.mol^{-1}.cm^2)
[Ag(SNAC)$_2$]NO$_3$	184
[Cu(SNAC)$_2$Cl$_2$]	22.4
[Co(SNAC)$_2$Cl$_2$]	84.5
[Pt(SNAC)$_2$Cl$_2$]Cl$_2$.H$_2$O	315
[Pd(SNAC)$_2$]Cl$_2$	290

Applications

Survey in antibacterial activity of synthesized ligand and its complexes

The biological activity for the ligand (SNAC) and its complex was studied against two selected types of bacteria *Escherichia Coil* (Gram-negative) and *Staphylococc -us aureus* (Gram-Positive). Water was utilized as a solvent and as a control, the solution concentration was [10^{-3}]mole. Amoxicillin was utilized as standard material to make a comparison of its effectiveness with that of

the synthesized compounds. The zone of inhibition of bacteria growth around the disc was controlled. Figures 24 and 25 and Table 10 list the deactivation capacity against the bacteria swap of the ligands (SNAC) and its complex. The results of the present study show that they had different deactivating capacity against the two types of selected bacteria as explained below: For *Escherichia Coil*:-[Co(SNAC)$_2$Cl$_2$]> SNAC > [Pt(SNAC)$_2$Cl$_2$]Cl$_2$.H$_2$O > [Cu(SNAC)$_2$Cl$_2$]> [Pd(SNAC)$_2$]Cl$_2$> [Ag(SNAC)$_2$]NO$_3$.

For *Staphylococcus aureus* [Pd(SNAC)$_2$]Cl$_2$> SNAC> [Co(SNAC)$_2$Cl$_2$] > [Cu(SNAC)$_2$Cl$_2$]> [Pt(SNAC)$_2$Cl$_2$]Cl$_2$.H$_2$O>[Ag(SNAC)$_2$]NO$_3$.

The metal complexes appeared higher activity. This is due to an increase inlipophilic nature which could be explained according to overtone's concept and tweedy's chelation theory [36]. Cell permeability and the lipid membrane that surrounds the cell, which favors the passage of only lipid-soluble material due to liposolubility, were thought to be the controlling factors in antibacterial activity. The positive charge of the metal ion is partially shared with the ligand donor atom in coordination, resulting in electron delocalization throughout the coordination ring [37].

TABLE 10 Inhibition activity rate of SNAC ligand against and its complexes

	Compounds	Gram Negative *Escherichia Coli (E-Coli)*	Gram Positive *Staphylococcus aureus*
	Amoxicillin	15	20
1	[Ag(SNAC)$_2$]NO$_3$	10	12
2	[Cu(SNAC)$_2$Cl$_2$]	12	19.5
3	[Co(SNAC)$_2$Cl$_2$]	24.5	19.7
4	[Pt(SNAC)$_2$Cl$_2$]Cl$_2$.H$_2$O	14	14.5
5	[Pd(SNAC)$_2$]Cl$_2$	11.5	20.5
6	SNAC	16.5	20
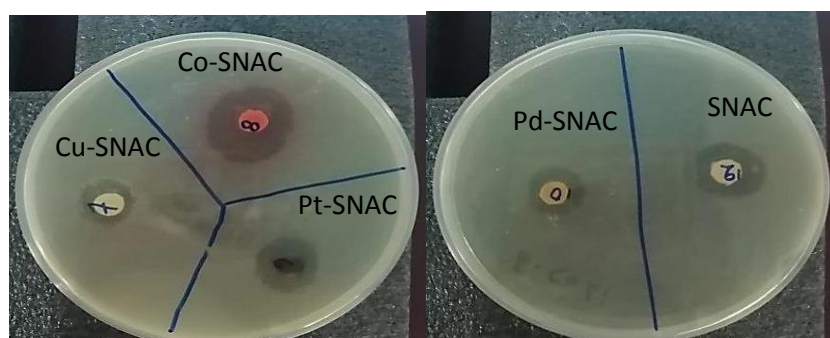
FIGURE 24 The inhibition zones versus bacterial gram negative (E.coil) for the SNAC and its complex
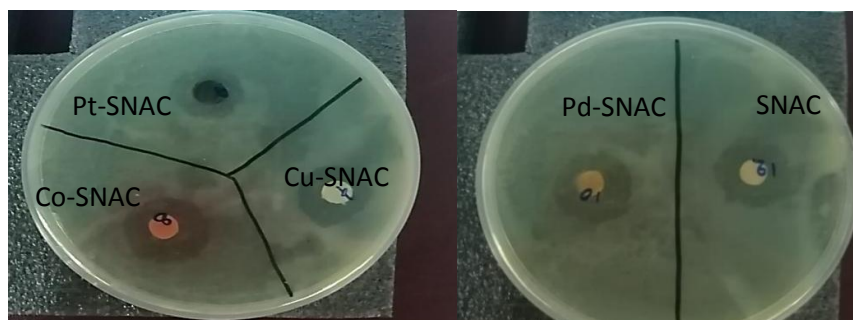
FIGURES 25 The inhibition zones versus bacterial gram positive (Staphylococcus aureus) ligand SNAC and its complex

Burns skin in mice

To assess burns healing activity of [Co(SNAC)$_2$Cl$_2$], four mice groups were tested. Mice hair was removed by hair removal cream (veet) and flame was used to induce burns of skin; the recovery days calculated by determining days required for recovering were studied. The results were shown (Table 11) that had the ability [Co(SNAC)$_2$Cl$_2$] to heal burns in 13 days in comparison with sliver sulfadiazine and negative control, which require 16 days and 18 days to complete recoveration as was shown in Figure 26. The main reason to increase the anti-inflammatory activity in selected complexes due to presence Caffeine contains heterocyclic ring with highly effective as an anti-inflammatory as well as the presence of effective moieties on benzene and naphthalene ring [38].

TABLE 11 The recovery of burn healing in mice after different treatments

| Groups	Treatment	Period of recovery
1	[Co(SNAC)$_2$Cl$_2$]	Days 13
1	Without any treatment	Days 18
3	Sliver sulfadiazine	Days 16

1   **2**

B-(13dyes)3

FIGURE 26 (1) Represented inducing of burns. (2) Picture during the period of treatment with [Co(SNAC)$_2$Cl$_2$] (3) After healing

Dyeing

SNAC and its complex ligand was used to color wool textiles. The wool textile is made up of the protein keratin (Scheme 3), which is made up of long polypeptide chains made up of 18 different amino acids with the general formula [$H_2N.CHR.COOH$], where [R] is a side chain with a different character and the chains are linked by bridges made up of cysteine.

Figure 27 showed woolen textile dyed with synthesized azo ligand and their selected complexes which their dyeing feature are listed in Table 12. These compounds were given a wide range of colors varying form yellow, orange, pink, and green to brown with good brightness, levelness and depth on the textile, the dyes were tested for light and detergent fastness. The difference in the shades of the azo dye textile results from both the position of the substituted present on the diazotized compound and the nature. In addition, the results for the selected complexes were compared according to gray scale, where 4-5 are considered good, 3 are moderate, and 1-2 are not good. According to Iraqi specifications No. 3616 for woolen textile, the models were dyed with a fixative at 260 °C for 30 minutes. The color fastness of the textiles was tested for washing with soap powder at a concentration of 2 %. The excellent fastness to wet and dry abrasion, while excellent to light fastness for staining and color change.
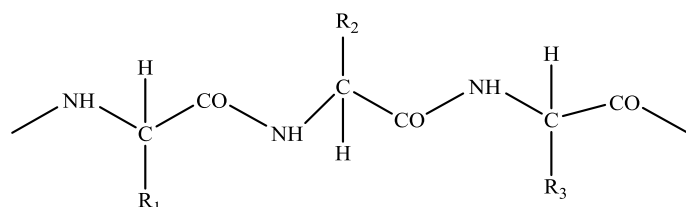
SCHEME 3 structure of protein keratin

TABLE 12 Results of dyeing and various fastness feature of some azo complexes on wool textile

Number of compounds	Color	Textile color fastness to wet and dry abrasion		Textile color fastness check for washing	
		dry rubbing	wet rubbing	staining with dye	color change
(Co-SNAC)	pink	4	4	5	3
(Pt-SNAC)	Green to brown	5	5	5	1
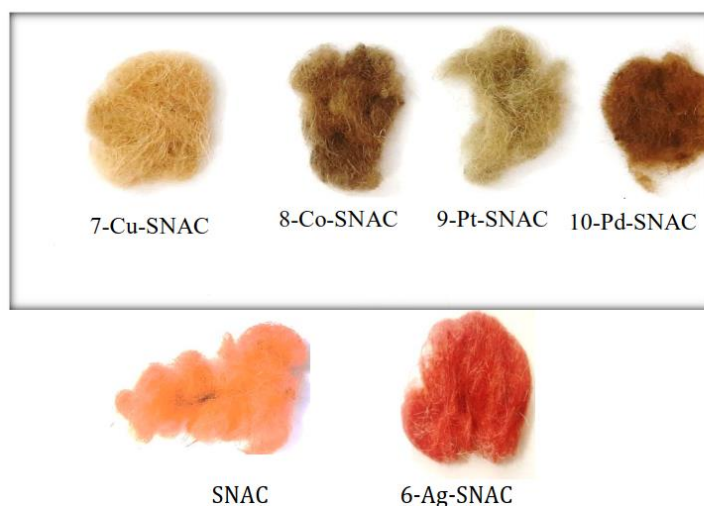
FIGURE 27 The dying of ligand and SNAC and some their complex

Anti-oxidant and radical scavenging activity

The in vitro antioxidant activity of the compound $[Pd(SNAC)_2]Cl_2$ was evaluated by DPPH (1,1-diphenyl-2-picrylhydrazyl) radical scavenging method. Ascorbic acid was used as the positive control [39].

Reductive ability

Ability to reduce the absorbance of $[Pd(SNAC)_2Cl_2]$ was considerably greater than trolox (vitamin E) at all concentrations tested (0.08, 0.16, 0.32, and 0.64 mg/mL), implying that the compounds are more effective than trolox in the reductive ability, which was concentration-dependent. It was (0.832±0.013) for $[Pd(SNAC)_2Cl_2]$ when the methanol extract concentration was 0.08 mg/mL, and it was increased dramatically to (2.056±0.018) when the concentration was 0.64 mg/mL (Table 13).

TABLE 13 Reductive ability of $[Pd(SNAC)_2]Cl_2$ and trolox (vitamin E)

Concentration (mg/mL)	Reductive Ability Absorbance (Mean ± SD)	
	$[Pd(SNAC)_2]Cl_2$	Trolox (Vitamin E)
0.08	0.832±0.013	**0.108 ± 0.001**
0.16	1.087±0.002	**0.114 ± 0.004**
0.32	1.493±0.005	**0.132 ± 0.007**
0.64	**2.056±0.018**	**0.211 ± 0.015**

Vitamin C also showed variations between the five concentrations (Table 14).

TABLE 14 DPPH radical scavenging activity of $[Pd(SNAC)_2]Cl_2$ and vitamin C

Concentration (mg/mL)	DPPH Radical Scavenging Activity (Mean ± SD; %)	
	$[Pd(SNAC)_2]Cl_2$	Vitamin C
12.5	23.77±1.335	**39.66 ± 2.52**
25	27.28±8.219	**41.33 ±10.01**
50	33.61±7.502	**48.33 ± 8.50**
100	37.05±5.027	**53.00 ±10.53**
200	**49.44±4.181**	**65.01±11.73**
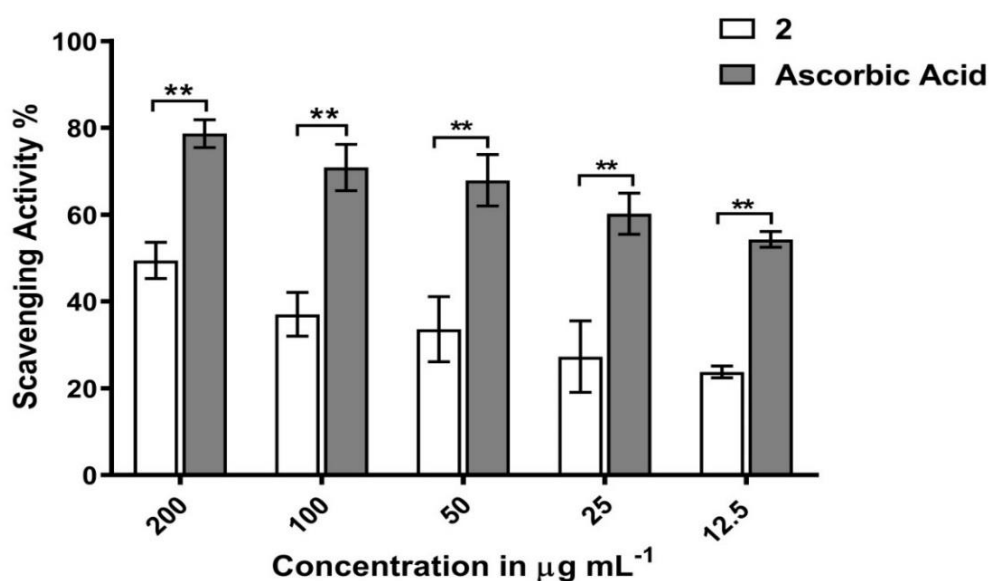
FIGURE 28 DPPH Radical scavenging activity of Pd(SNAC)$_2$]Cl$_2$

Survey in anticancer effectiveness

Cytotoxic effect of [Cu(SNAC)₂Cl₂] in Vitro using MTT assay

The cytotoxic impact of [Cu(SNAC)$_2$Cl$_2$] on colon cancer cell line was determined using 3-(dimethylthiazol-2-yl)-2,5-diphenyltetrazolium bromide (MTT) (CACO2). The MTT assay was used to determine cell viability and inhibition rate on the tumor cell line by using different concentrations of the complex [Cu(SNAC)$_2$Cl$_2$]. The percentage viability of treated cells was calculated in a comparison with normal cell line WPL-68 [40]. The cytotoxic effect of [Cu(SNAC)$_2$Cl$_2$] in a concentration range from 6.2-400 μg/ mL on CACO-2 cells line (Table 15) demonstrated a dose-dependent decrease in cell viability. By increasing the concentration of [Cu(SNAC)$_2$Cl$_2$], cell viability is lowered. The lowest CACO2 cell viability (percentage) was observed at 400 g/ mL (45.767.33), while the maximum CACO2 cell viability was observed at 6.2 g/ mL (94.75 1.80). With an IC50 of (222.5) g/ mL, [Cu(SNAC)$_2$Cl$_2$] was shown to have the most effective cytotoxic action. The action of [Cu(SNAC)$_2$Cl$_2$]on WRI-68 normal cell line, on the other hand, yielded an IC50 of (47.44) g/ mL (Figure 30). Through the values of IC50, we conclude that the Copper complex needs a low concentration to kill CACO-2 cell line and at the same time its effect is felt on normal cell (WRL-68).

TABLE 15 Cytotoxicity effect of [Cu(SNAC)$_2$Cl$_2$] on CACO2 and WRI-68 cells after 24 hours incubation at 37 °C

[Cu(SNAC)₂Cl₂] (μg/mL)	CACO2 cell line viable cell count Mean± S.D.	WRL-68 cell line's viable cell count Mean± S.D.
400.00	45.76 ±7.33	72.69 ±1.71
200.00	51.35 ±1.34	84.49 ±1.80
100.00	54.51 ±1.97	93.06 ±2.34
50.00	70.95 ±7.98	93.79 ±0.58
25.00	85.30 ± 7.63	93.48 ±1.36
12.50	96.10 ±0.59	95.10 ±1.97
6.25	94.75 ±1.80	94.29 ±1.17
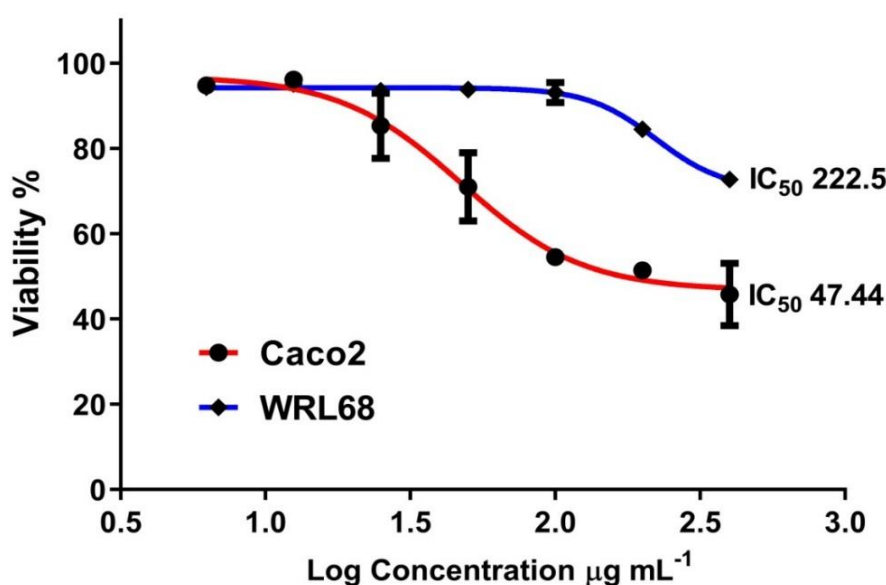
FIGURE 30 Cytotoxic effect of [Cu(SNAC)$_2$Cl$_2$] on CACO2 and WRL-68 cells after a 24-hour incubation period at 37 degrees celsius

Acid - base indicator

Azo dyes consider one of the most commonly used compounds as indicators, due to having sequer of π delocalization and have vivid colors especially yellow, red and orange [41].

The ligand (SNAT) was utilized as indicators in acid _ base titration by used (0.1M) of HC1 aginst (0.1M) NaOH and (0.1M) of CH_3COOH against (0.1M) of NaOH. The ligand having clear color in acidic or basic solution gives sharp color change when moving from the acidic to basic solution as was shown in Figure 30 and all data was collected in Table 16.

TABLE 16 Titration of acid (0.1M) against NaOH (0.1M) for (SNAC)

No	Volume of acetic acid	Volume of NaOH	Color in acid	Color in base
1	(HCl) 5 mL	8mL	brown	red
2	(ACOH) 5 mL	10mL	pink	Light yellow
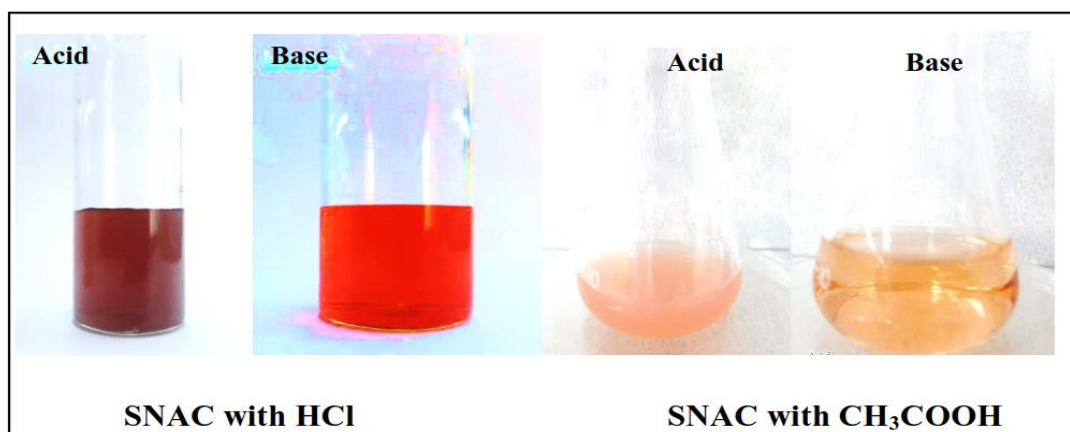
FIGURE 30 Change in color of Azo ligand (SNAC) in acid and base solutions

Conclusion

1- The coupling reaction of diazonium salt with Caffeine yielded new azo ligand ANAC, which was confirmed by analytical physicochemical studies.

2- The ligand SNAC acted as neutral N,N-bidentate chelating ligand when was interacted with [Ag(I), Co(II), Pt(IV) and Cu(II),Pd(II)] through the azo nitrogen and the imidazole nitrogen in Caffeine moiety which have pentagonal chelating ring. Link sites have been identified between the ligand and metal ions.

3- The electronic, FTIR, and ¹HNMR spectra of the complexes revealed a great change compared to the free ligand spectra.

4- Electronic spectra and magnetic moment data for the complexes proposed octahedral geometry for [Ag(I), Co(II), Pt(IV) Pd(II)] complexes, while the Cu(II) complex has distorted octahedral (D_4h).

5- The ligand and its complexes have different effectiveness antibacterial, antioxidant, anticancer activity and Burns healing.

6- The ligand and its complexes have various colors that were confirmed to dying wool and the ligands acts as an acid-base indicator.

Orcid:

Alyaa Khider Abbas: https://orcid.org/0000-0002-8400-0926

References

[1] E.W.C. Chan, S.K. Wong, J. Tangah, H.T. Chan, *Sys. Rev. Pharm.,* **2018**, *9*, 58-63. [Pdf], [Google Scholar], [Publisher]

[2] Z.Y. Kadhim, A.N. Seewan, M.T. Abd, H.R. Saud, *Int. J. Pharm. Res.,* **2020**, *12*, 402-407.[crossref], [Google Scholar], [Publisher]

[3] M. Mohorčič, J. Friedrich, A. Pavkob, *Acta Chim. Slov,* **2004**, *51*, 619-628. [Pdf], [Google Scholar], [Publisher]

[4] S. Piotto, S. Concilio, L. Sessa, R. Diana, G. Torrens, C. Juan, U. Caruso, P. Iannelli, *Molecules,* **2017**, *22*, 1372. [crossref], [Google Scholar], [Publisher]

[5] N.M. Mallikarjuna, J. Keshavayya, M.R. Maliyappa, R.A.S. Ali, T. Venkatesh, *Journal of Molecular Structure,* **2018**, *1165*, 28-36. [crossref], [Google Scholar], [Publisher]

[6] A. Shridhar, J. Keshavayya, S. Peethambar, H. J. Hoskeri, *Arab. J. Chem.,* **2016**, *9*, S1643-S1648. [crossref], [Google Scholar], [Publisher]

[7] M. Maliyappa, J. Keshavayya, N. Mallikarjuna, P.M. Krishna, N. Shivakumara, T. Sandeep, K. Sailaja, M.A. Nazrulla, *J. Mol. Struct.,* **2019**, *1179*, 630-641. [crossref], [Google Scholar], [Publisher]

[8] G. Hussain, N. Abbas, M. Ather, M.U.A. Khan, A. Saeed, R. Saleem, G. Shabir, *J. Chin. Chem. Soc.,* **2016**, *63*, 645-652. [crossref], [Google Scholar], [Publisher]

[9] C. Esimone, F. Okoye, C. Nworu, and C. Agubata, *Trop. J. Pharm. Res.,* **2008**, *7*, 969-974. [crossref], [Google Scholar], [Publisher]

[10] T. Hashimoto, Z. He, W.Y. Ma, P.C. Schmid, A.M. Bode, C.S. Yang, Z. Dong, *Cancer Res.,* **2004**, *64*, 3344-3349. [crossref], [Google Scholar], [Publisher]

[11] G.B. Keijzers, B.E. De Galan, C.J. Tack, P. Smits, *Diabetes Care,* **2002**, *25*, 364-369. [crossref], [Google Scholar], [Publisher]

[12] E. Grucka-Mamczar, J. Zalejska-Fiolka, D. Chlubek, S. Kasperczyk, U. Błaszczyk, A. Kasperczyk, E. Swietochowska, E. Birknera, S. Poland, *Fluoride,* **2009**, *42*, 105-109. [Pdf], [Google Scholar], [Publisher]

[13] H. Hosseinzadeh, B.B. Fazli, S.M. Moaddab, *Iranian Biomedical Journal*, **2006**, *10*, 163-167. [Google Scholar], [Publisher]

[14] E. Ibezim, C. Esimone, P. Nnamani, I. Onyish, S. Brown, C. Obodo, *Afr. J. Biotechnol.,* **2006**, *5*, 1781-1784. [Pdf], [Google Scholar], [Publisher]

[15] L.M.L. Ogboji, O.Z. Esezobor, M.E. Khan, J.O. Igoli, *Chem. Sci. Int. J.,* **2017**, *20*, 1-5. [Pdf], [Google Scholar], [Publisher]

[16] Ö. Altun, M. Şuözer, *J. Coord. Chem.,* **2019**, *72*, 2091-2105. [crossref], [Google Scholar], [Publisher]

[17] S. Puig, D.J. Thiele, *Curr. Opin. Chem. Biol.,* **2002**, *6*, 171-180. [crossref], [Google Scholar], [Publisher]

[18] W. Fu, J. Chen, Y. Cai, Y. Lei, L. Chen, L. Pei, D. Zhou, X. Liang, J. Ruan, *J. Ethnopharmacol.,* **2010**, *130*, 521-528. [crossref], [Google Scholar], [Publisher]

[19] C.K. Lim, W.N Tiong, J.L. Loo, *Int. J. Phytopharm.,* **2014**, *4*, 01-05. [crossref], [Google Scholar], [Publisher]

[20] M.F. Kamaruddin, M.Z. Hossain, A. Mohamed Alabsi, M. Mohd Bakri, *Medicina,* **2019**, *55*, 322. [crossref], [Google Scholar], [Publisher]

[21] G.J. Brewer, *J. Am. Coll. Nutr.,* **2009**, *28*, 238-242. [crossref], [Google Scholar], [Publisher]

[22] D.A. Skoog, F.J. Holler, S.R. Crouch, *Principles of instrumental analysis*, Cengage learning, **2017**. [Google Scholar], [Publisher]

[23] H.W. Gao, J.F. Zhao, *Croatica Chemica Acta,* **2003**, *76*, 1-6. [Pdf], [Google Scholar], [Publisher]

[24] N.M. Rageh, *Spectrochim. Acta A Mol. Biomol. Spectrosc.,* **2004**, *60*, 1917-1924. [crossref], [Google Scholar], [Publisher]

[25] A.A. Alothman, Z.M. Almarhoon, *J. Mol. Struct.,* **2020**, *1206*, 127704. [crossref], [Google Scholar], [Publisher]

[26] Y. Issa, W. El-Hawary, A. Youssef, A. Senosy, *Spectrochimica Acta Part A: Molecular and Biomolecular Spectroscopy,* **2010**, *75*, 1297-1303. [crossref], [Google Scholar], [Publisher]

[27] H.A. Bayoumi, A. Alaghaz, M.S. Aljahdali, *Int. J. Electrochem. Sci,* **2013**, *8*, 9399-9413. [Pdf], [Google Scholar], [Publisher]

[28] H. Dinçalp, F. Toker, İ. Durucasu, N. Avcıbaşı, S. Icli, *Dyes Pigm.,* **2007**, *75*, 11-24. [crossref], [Google Scholar], [Publisher]

[29] A. Abbas, R.S. Kadhim, *J. Appl. Chem.,* **2016**, *9*, 20-31. [crossref], [Google Scholar], [Publisher]

[30] M. Mohamed, C. Janowitz, I. Unger, R. Manzke, Z. Galazka, R. Uecker, R. Fornari, J.R. Weber, J.B. Varley, C.G. Van de Walle, *Appl. Phys. Lett.,* **2010**, *97*, 211903. [crossref], [Google Scholar], [Publisher]

[31] E. Yohannes, B. Chandravarishi, R.K. Gridasova, *Bull. Chem. Soc. Ethiop.,* **1995**, *9*, 1-8. [Pdf], [Google Scholar], [Publisher]

[32] N.M. Aljamali, *Int. J. Med. Pes. Pharm. Sci.,* **2015**, *2*, 28-36. [Pdf], [Google Scholar], [Publisher]

[33] M. Tuncel, *Asian J. Chem.*, **2014**, *26*, 2161-2165. [crossref], [Google Scholar], [Publisher]

[34] K.J. Al-Adilee, H.K. Dakheel, *Eurasian J. Anal. Chem.,* **2018**, *13*, ID: 59389396. [crossref], [Google Scholar], [Publisher]

[35] J.C. Espinosa, S. Navalón Oltra, A.M. Primo Arnau, M. Moral, J. Fernandez Sanz, M.M. Alvaro Rodríguez, H. García, *Chem. Eur. J.,* **2015**, *21*, 11966-11971. [crossref], [Google Scholar], [Publisher]

[36] S. Belaid, A. Landreau, S. Djebbar, O. Benali-Baitich, G. Bouet, J.P. Bouchara, *J. Inorg. Biochem.,* **2008**, *102*, 63-69. [crossref], [Google Scholar], [Publisher]

[37] R. Nair, A. Shah, S. Baluja, S. Chanda, *J. Serbian Chem. Soc.,* **2006**, *71*, 733-744. [crossref], [Google Scholar], [Publisher]

[38] L. Rodas, A. Riera-Sampol, A. Aguilo, S. Martínez, P. Tauler, *Nutrients,* **2020**, *12*, 2325. [crossref], [Google Scholar], [Publisher]

[39] S. Hamza Sherif, B. Gebreyohannes, *J. Chem.,* **2018**, *2018*, Article ID 4032105. [crossref], [Google Scholar], [Publisher]

[40] A. Taş, S. Şahin-Bölükbaşı, E. Çevik, E. Özmen, E. Gümüş, Y. Siliğ, *Indian J. Pharm. Educ. Res,* **2018**, *52*, S119-S123. [crossref], [Google Scholar], [Publisher]

[41] B. Purwono, C. Anwar, A. Hanapi, *Indones. J. Chem.,* **2013**, *13*, 1-6. [crossref], [Google Scholar], [Publisher]